BIOSENOSRS

BIO 580

Nanobiosensors

WEEK-13

Fall Semester

Faculty: Dr. Javed H. Niazi KM
Faculty of Engineering & Natural Sciences
Sabanci University

Topics that will be covered in the course

- ❑ History of biosensor development, applications and requirements of biosensors and classification
- ❑ Principles of molecular recognition and transduction signal acquisition
  - ✓Sources of Biological Recognition elements – enzymes/proteins, ssDNAs, antibody and Others
  - ✓Design considerations for use of recognition elements in biosensors
  - ✓Modeling of reactions for various biosensor applications- electrochemical, optical, piezoelectric, colorimetric, fluorometric and others.
- ❑ Modification of sensor surfaces and immobilization techniques
  - ✓Covalent modification of surfaces using surface chemistry
  - ✓Self Assembled Monolayers (SAM) and adsorptions
  - ✓Other ways to immobilize biological macromolecules on various solid surfaces
- ❑ Detection methods and Physical Sensors
  - ✓Electrodes/transducers – electrochemical (amperometric, potentiometric, and conductimetric transductions)
  - ✓Other sensors - for e.g., optical sensors (colorimetric/fluorimetric/luminometric sensors), Surface Plasmon Resonance (SPR) sensors, and piezoelectric resonators.
- ❑ Fabrication of biosensors
  - ✓Miniaturization-application of nano-materials, nanoparticles, carbon nanotubes (CNTs) and others
  - ✓Biocompatibility – stability, reproducibility and repeatability of biomolecules on transducer surfaces
- ❑ Data acquisition, statistical and error analysis
  - ✓Inter and Intra-assays and Coefficient of variation (CV)
  - ✓Signal to noise ratio
  - ✓Normalization/optimization and signal retrieval
- ❑ Examples of commercial biosensors

Development of NanoBioSensors

New-generation nano-engineered biosensors, enabling nanotechnologies and nanomaterials

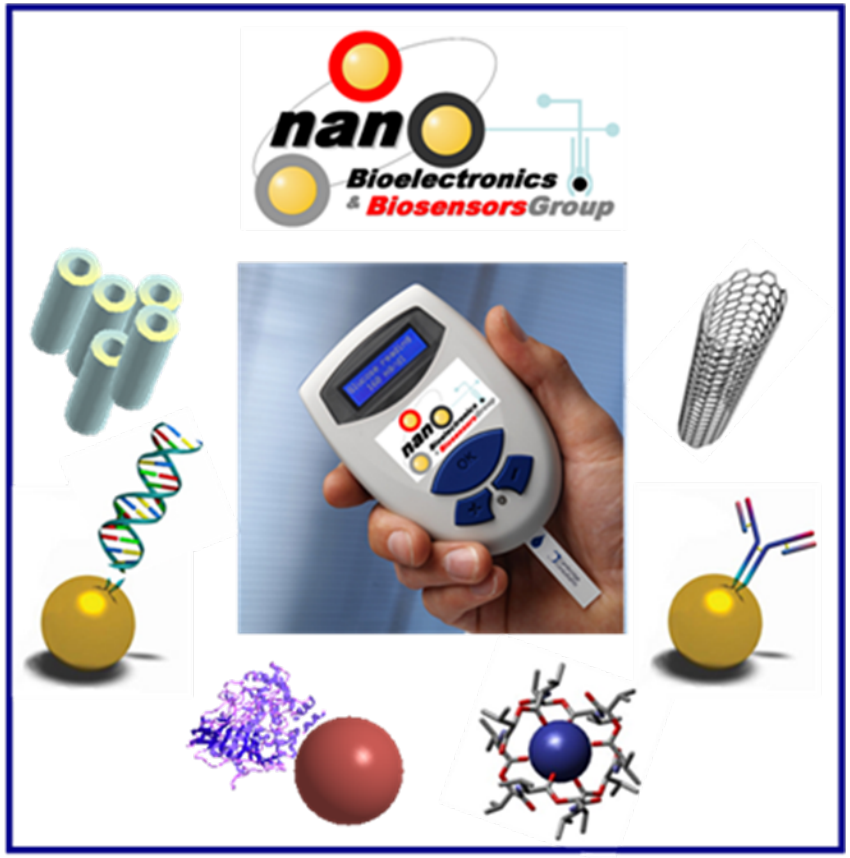

NANOSENSORS: Exploring the Sanctuary of Individual Living Cell: The combination of nanotechnology, biology, advanced materials and photonics opens the possibility of detecting and manipulating atoms and molecules using nano-devices, which have the potential for a wide variety of medical uses at the cellular level. Recently reported information showed the development of nano-biosensors and in situ intracellular measurements of single cells using antibody-based nanoprobes. The nano-scale size of this new class of sensors also allows for measurements in the smallest of environments. One such environment that has evoked a great deal of interest is that of individual cells. Using these nanosensors, it is possible to probe individual chemical species and molecular signaling processes in specific locations within a cell. Studies have shown that insertion of a nano-biosensor into a mammalian somatic cell not only appears to have no effect on the cell membrane, but also does not effect the cell's normal function. The possibilities to monitor in vivo processes within living cells could dramatically improve our understanding of cellular function, thereby revolutionizing cell biology.

Nanotechnology involves development of materials (and even complete systems) at the atomic, molecular, or macromolecular levels. The dimensional range of interest is approximately 1-500 nm.

In the field of biosensors, carbon nanotubes, the typical element of nanotechnology, have received considerable attention because of their

- inert properties
- conducting behaviour and
- high-surface area.

Particularly, their promotional ability for electron-transfer reactions with enzymes and other biomolecules has made carbon nanotubes the ideal supporting material for heterogeneous catalysts.

A carbon nanotube (CNT) is a tubular form of graphite sheet in nano dimensions.

A single-wall carbon nanotube (SWCNT), ranging in diameter from **0.4 to >3 nm**, can be visualized as formed by the rolling of a layer of graphite, called a graphene layer into a seamless cylinder.

Similarly, a multiwall carbon nanotube (MWCNT), ranging in diameter from **1.4 to >100 nm**, can be treated as a coaxial assembly of cylinders of SWCNTs

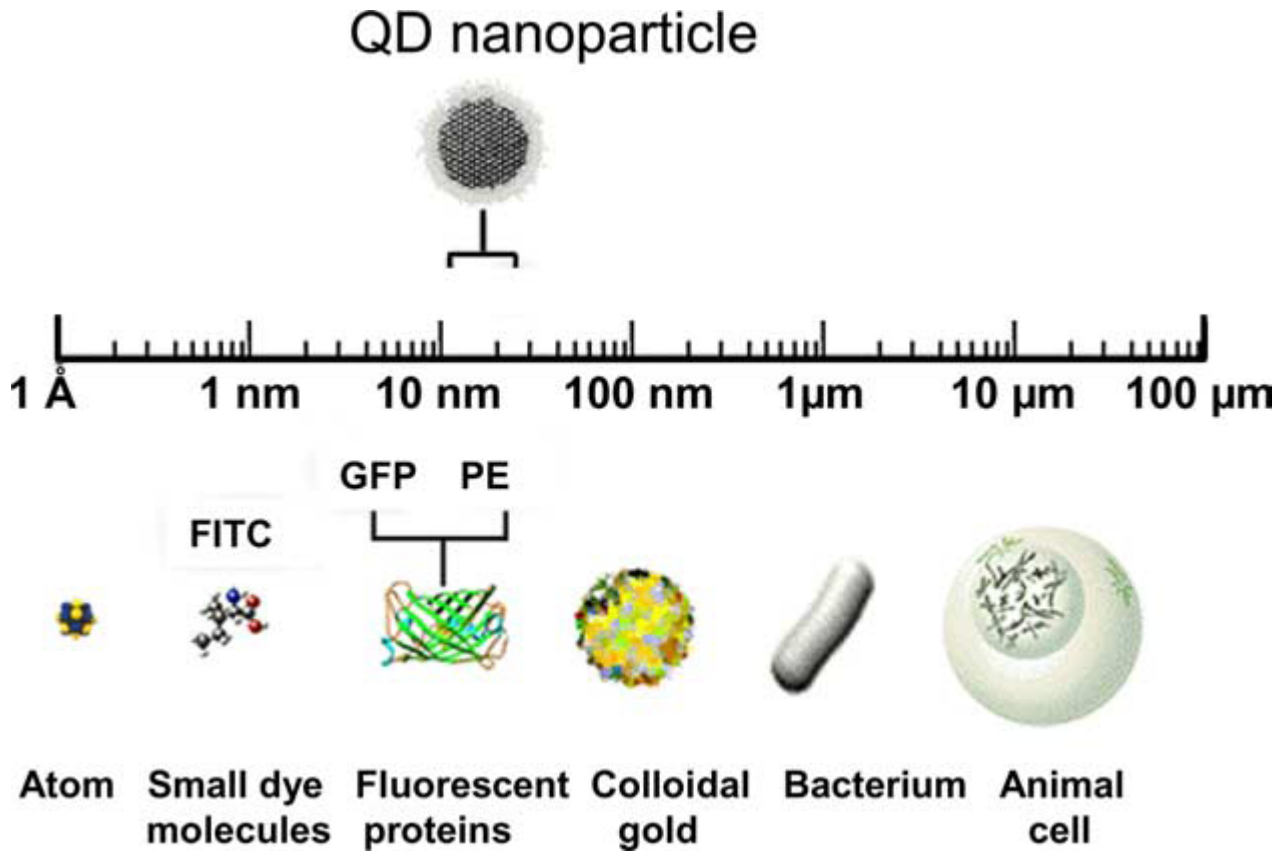

The size of a quantum dot (QD) compared to that of other materials. QD nanoparticle refers to quantum dots that have been solubilized and conjugated to affinity molecules. GFP, Green fluorescent protein; PE, Phycoerythrin; FITC, Fluoresceineisothiocyanate.

Spectrum, absorption and emission

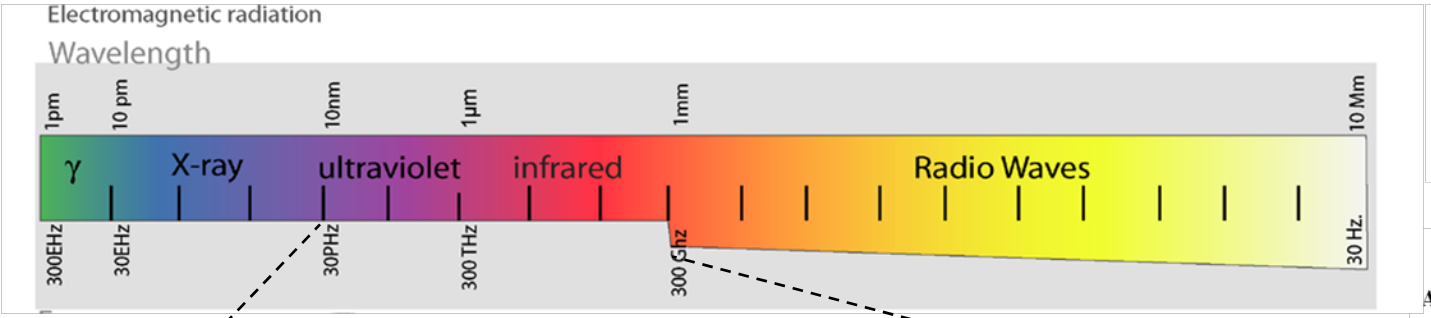

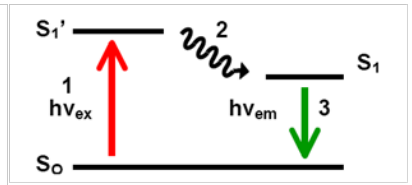

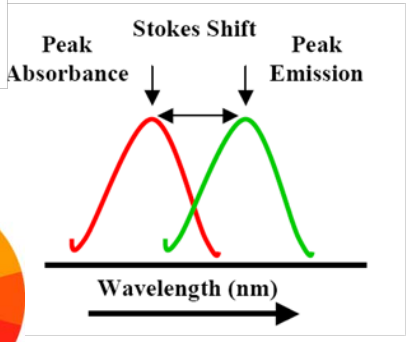

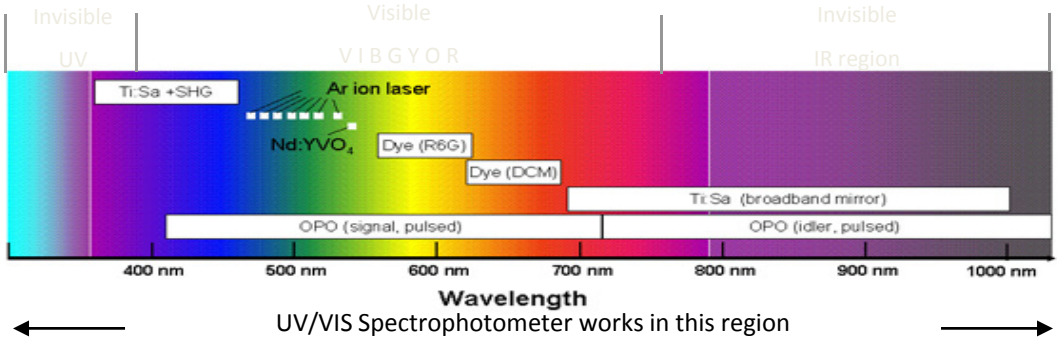

UV/VIS Spectrophotometer works in this region

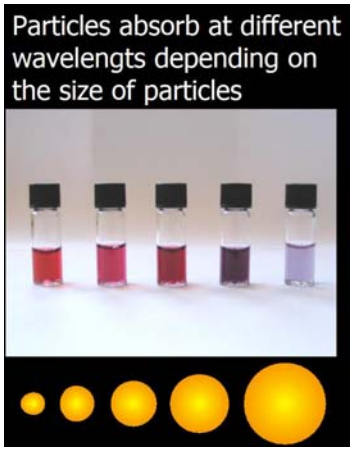

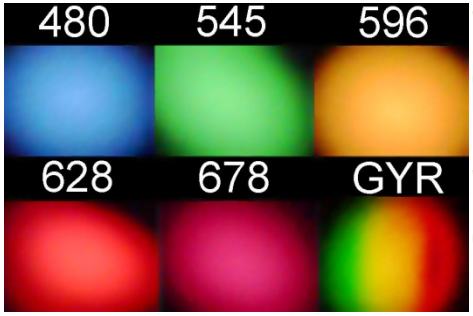

Wavelength (nm)

Color

Wavelength (nm)

Color

Examples

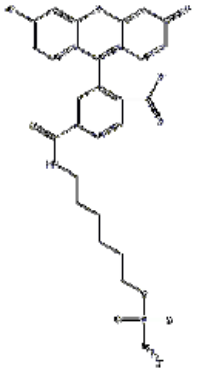

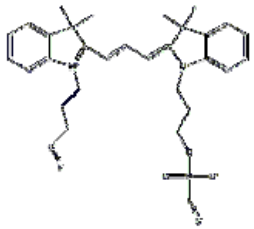

Cy3
(552/570)

Fluorescein
(492/520)

Brief Background

Exploiting properties of gold nanoparticles

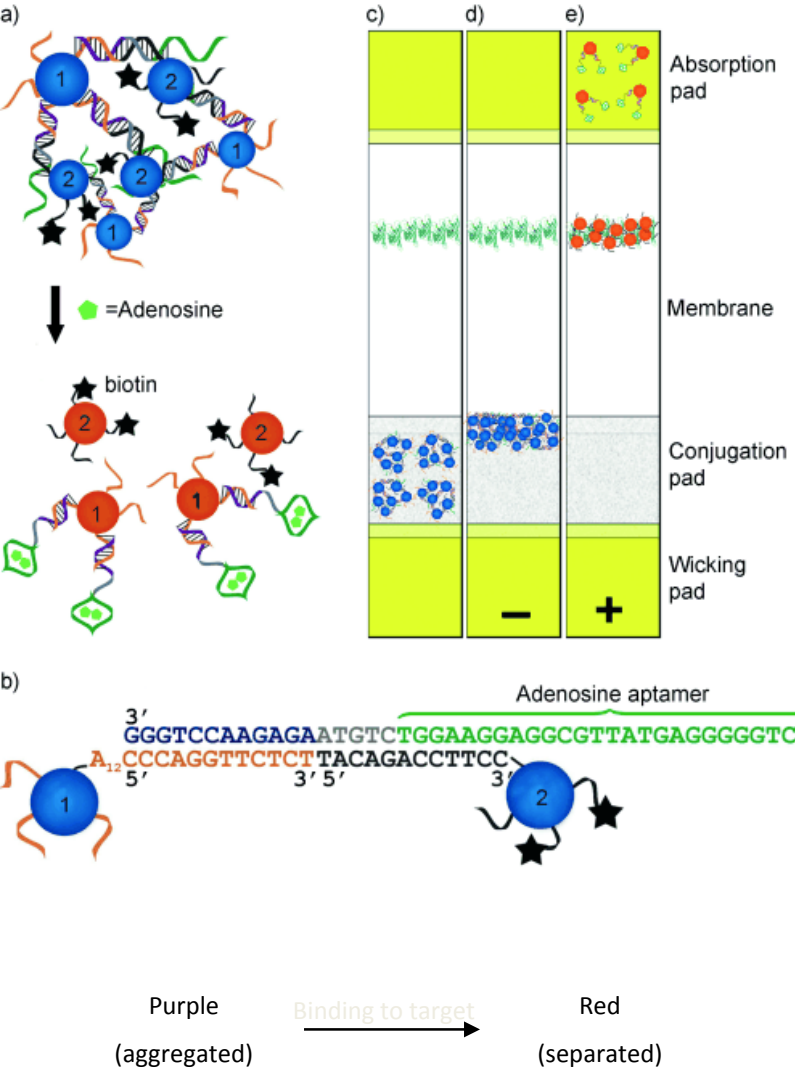

Aptamer/nanoparticle-based lateral flow device. a) Adenosine-induced disassembly of nanoparticle aggregates into red-colored dispersed nanoparticles. Biotin is denoted as black stars (*). b) DNA sequences and linkages in nanoparticle aggregates. Lateral flow devices loaded with the aggregates (on the conjugation pad) and streptavidin (on the membrane in cyan color) before use (c) and in a negative (d) or a positive (e) test.

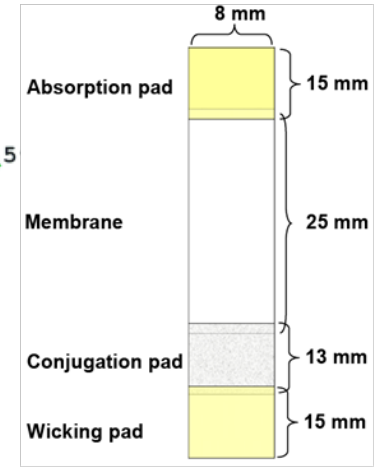

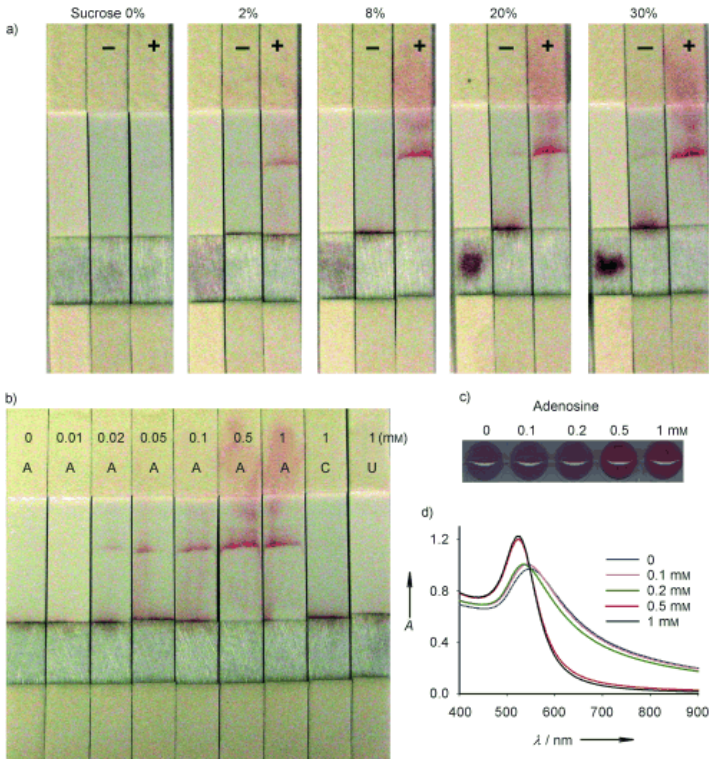

Fabrication of existing biosensors by bottom-up approach

The channel region and gate dielectric of an ISFET has been fabricated by layer-by-layer self-assembly technique, (Liu and Cui, 2007). The advantages of this approach are technological simplicity and the ability to produce low-cost sensors.

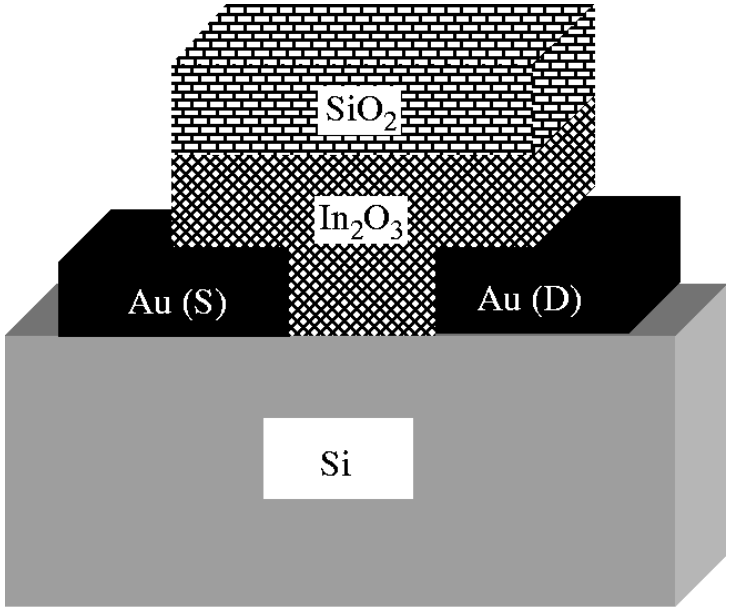

Notes: PDDA-poly (dimethyldiallyl-ammonium chloride), and PSS-poly(styrenesulfonate)

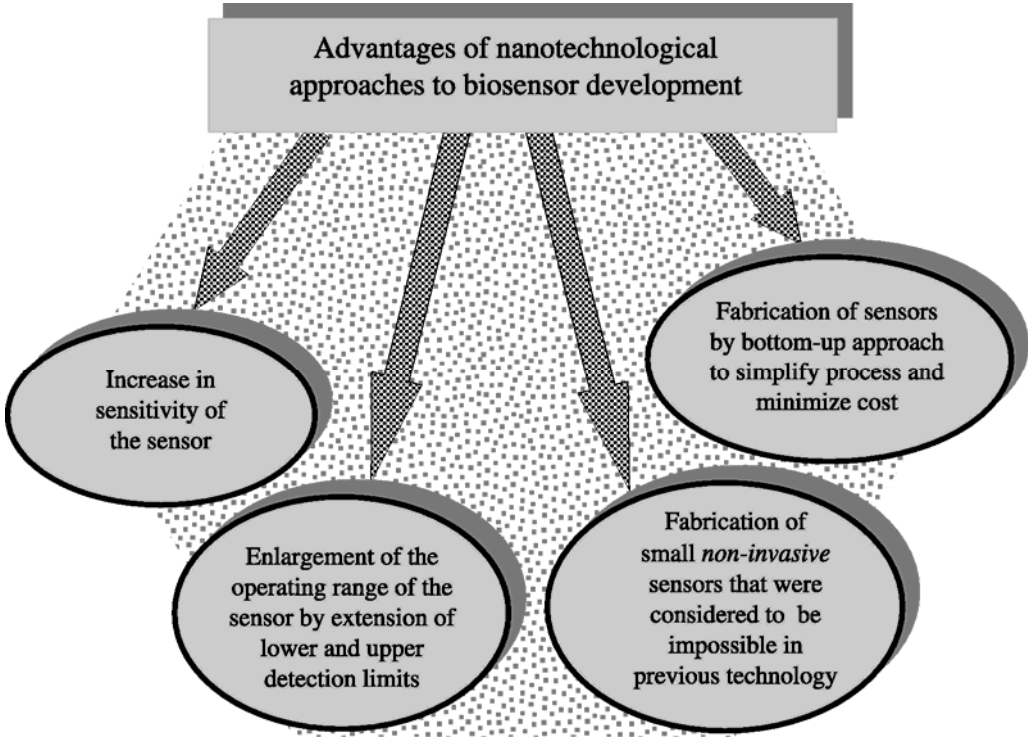

Main research activities are:

1. Design, preparation and characterization of nanomaterials for sensors and biosensors applications

2. Electrochemical sensors based on nanostructurated materials (i.e. carbon nanotubes etc.) for various monitoring and other industrial applications.

3. Nanoparticle based electrochemical detection (bio)systems and biosensors for DNA, protein and cell detection with interest for user-friendly diagnostics, security and quality control for various applications.

4. Fast and low cost sensing devices for heavy metals and other compounds with interest for environment control and other industrial applications.

5. Lab-on-a-chip systems with interest for in-field screening of analytes and other applications.

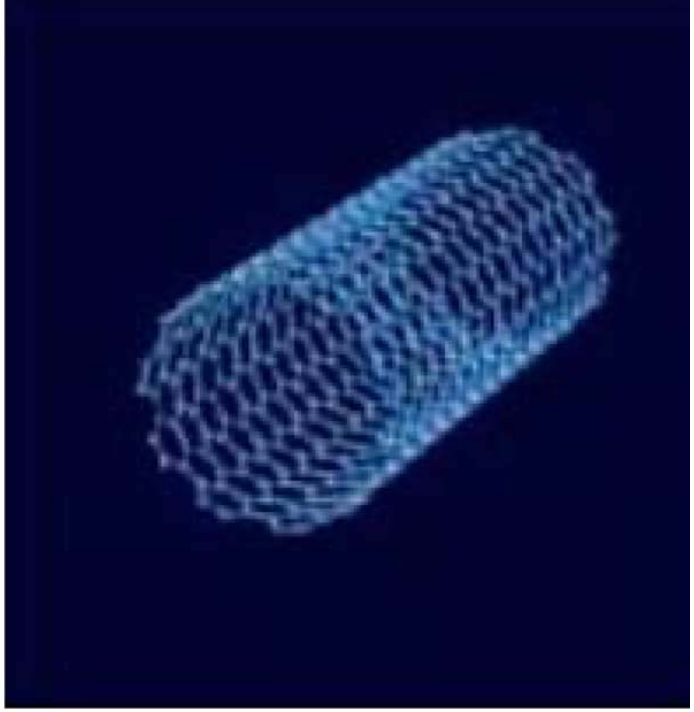

A

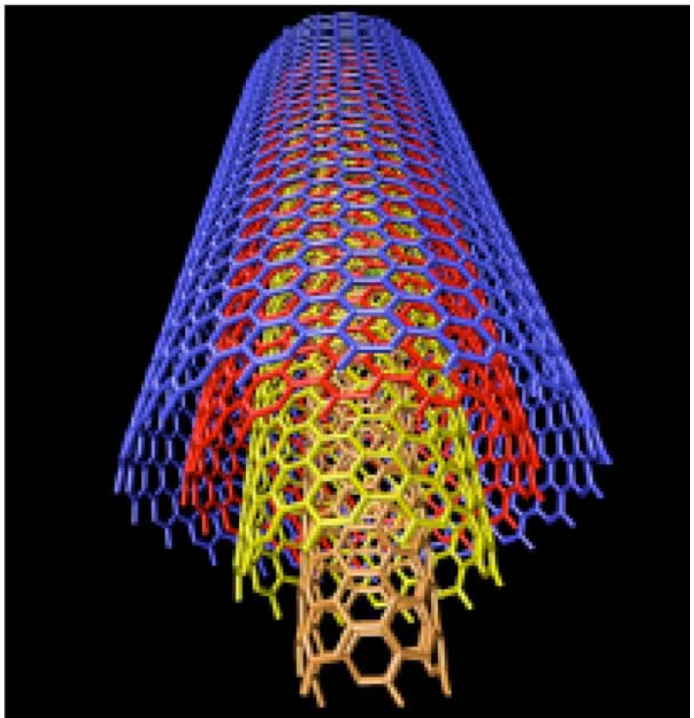

B

CARBON NANOTUBES CNTs

1. Carbon nanotubes (CNTs) combine in a unique way high electrical conductivity, high chemical stability and extremely high mechanical strength.

2. These special properties of both single-wall (SW) and multi-wall (MW) CNTs haveattracted the interest of many researchers in the field of electrochemical sensors.

3. Here, the latest advances and future trends in producing, modifying, characterizing and integrating CNTs into electrochemical sensing systems.

4. CNTs can be either used as single probes after formation *in situ* or even individually attached onto a proper transducing surface after synthesis.

5. Both SWCNTs and MWCNTs can be used to modify several electrode surfaces in either vertically oriented "nanotube forests" or even a non-oriented way.

6. They can be also used in sensors after mixing them with a polymer matrix to form CNT composites.

Nanomaterials: high aspect ratio

Carbon Nanotubes

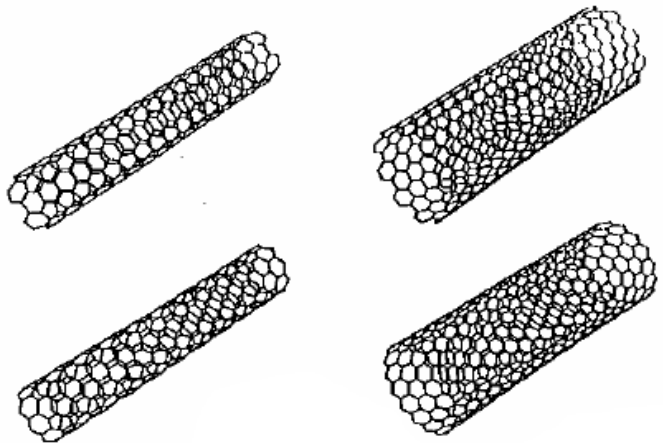

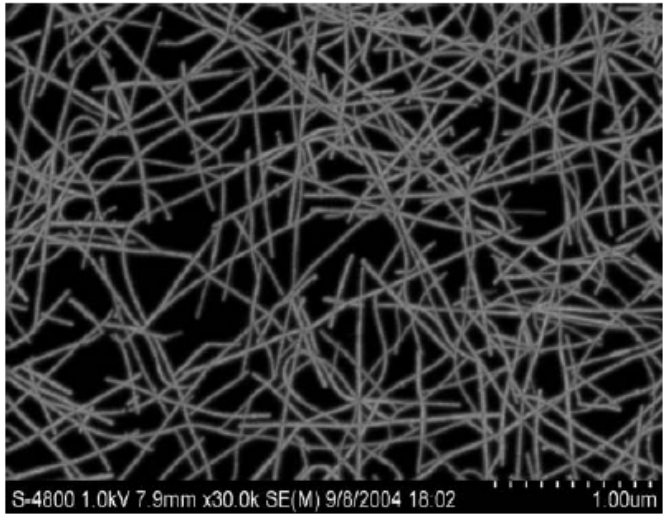

D=1-2nm L = 1- 5um

In_2O_3 Nanowires

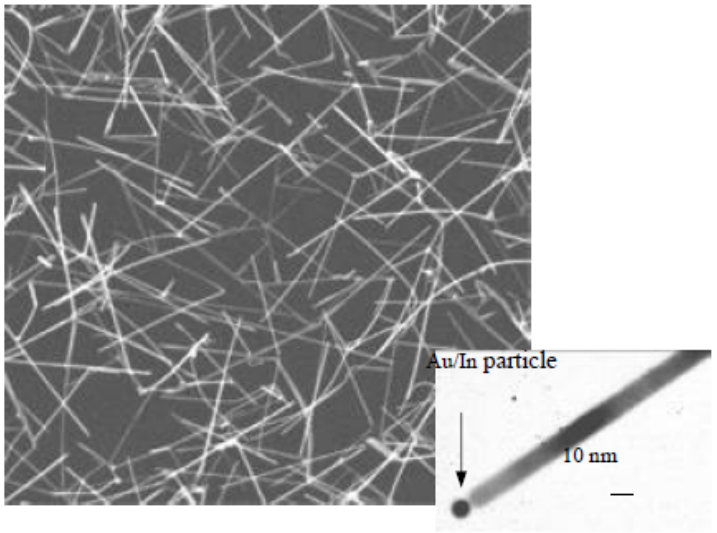

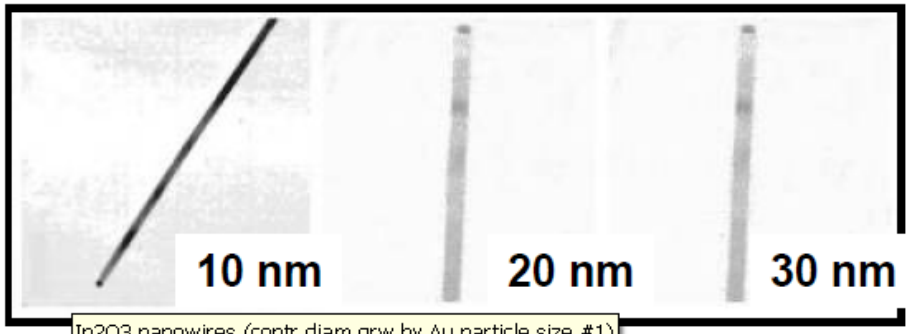

TEM image showing nanowire diameter controlled growth via Au particle size.

D=10-30nm L = 1- 5um

In_2O_3 Nanowire Field Effect Transistor (FET)

- 10 nm diameter Au clusters were used as catalyst

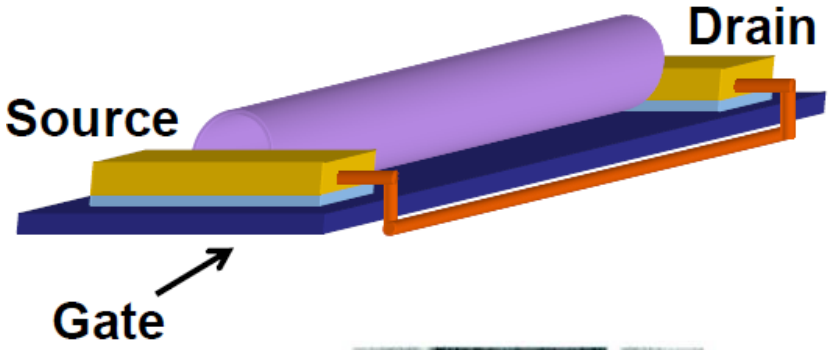

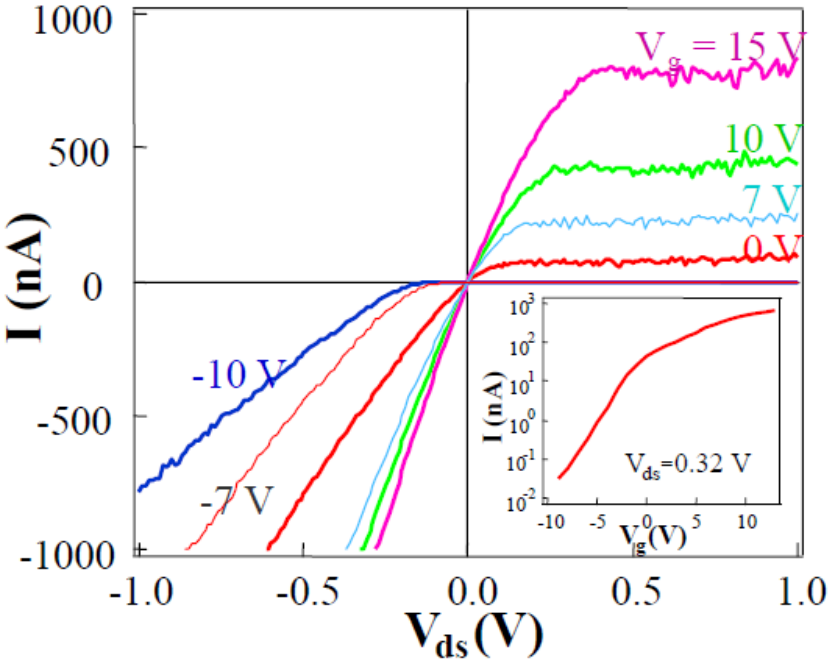

- V_g = gate voltage
- V_{ds} = source drain voltage
- Good gate dependence.
- on/off ratio = 10^4

This nanobiosensor consists of two microelectrodes connected by a bridge of nanotubes with antibodies. Since electrical signals produced by the union of a tumour with the sensor molecule biosensor it detects the appearance of a tumour.

C. Zhou, *et. al., Appl. Phys. Lett.* **2003**

FET based NanoBioSensor

Biorecognition agent: antibody, aptamer, oligonucleotide

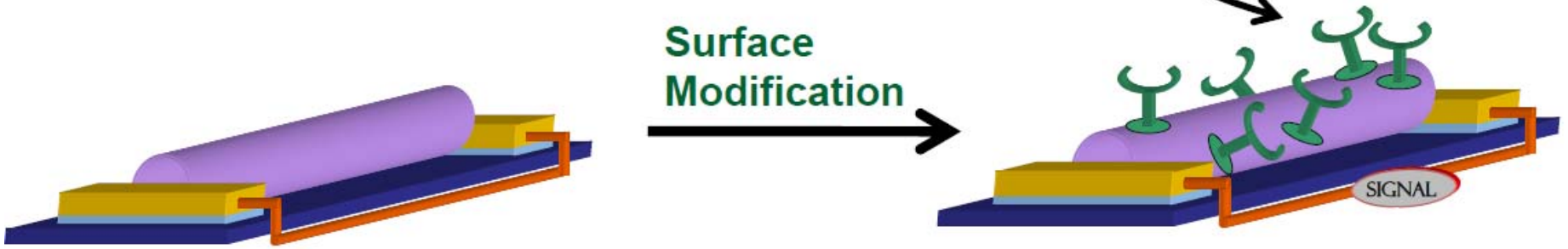

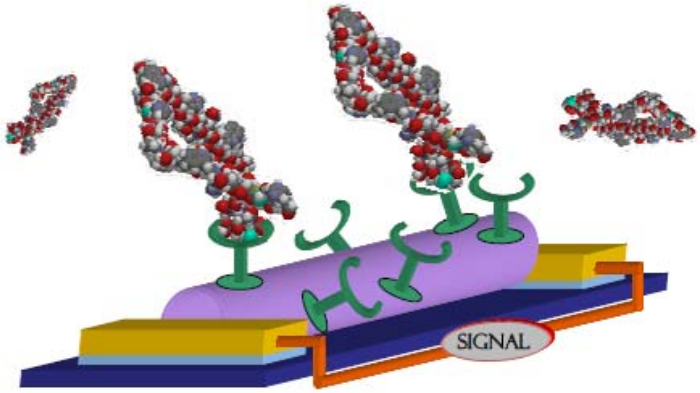

- Binding the bio-analyte changes properties of nanowire and the thus FET properties
- **Why nano?** High surface to volume ratio is critical for high sensitivity

Surface Treating NanoBioSensors: Prostate-Specific Antigen (PSA) sensors

Two different linking molecules are required to attach PSA antibody to the NW/SWNT surface:

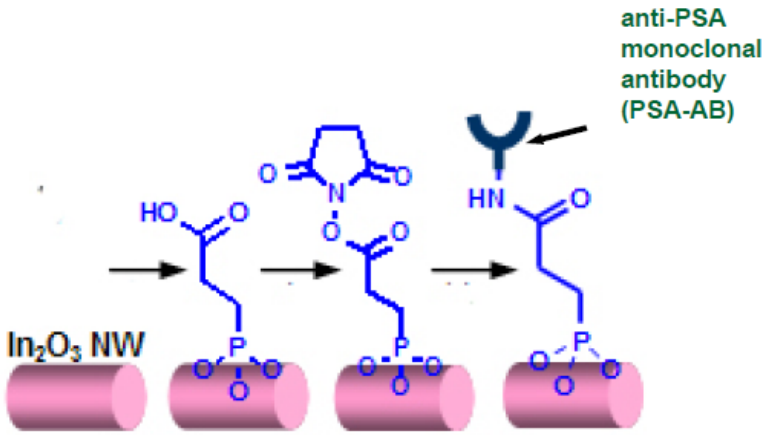

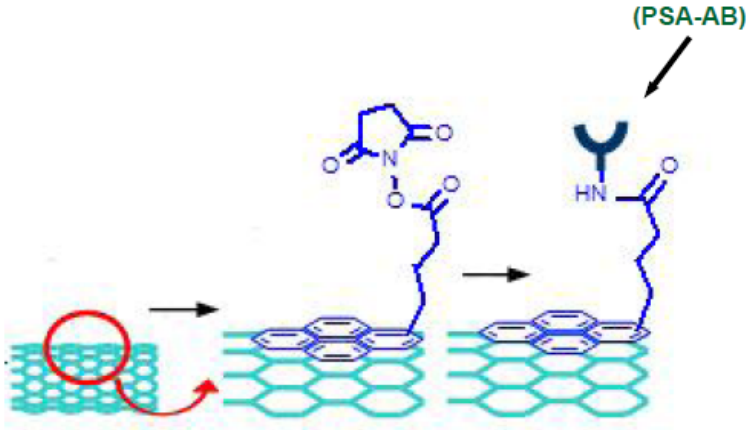

In_2O_3 nanowire

Single walled carbon nanotube

PSA Detection with Bionanosensor

In_2O_3 NW Device

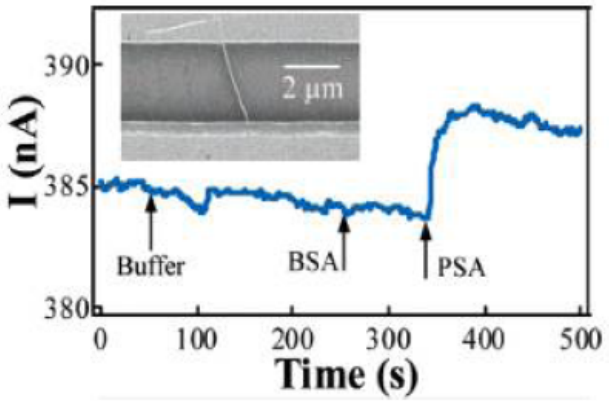

SWNT Mat Device

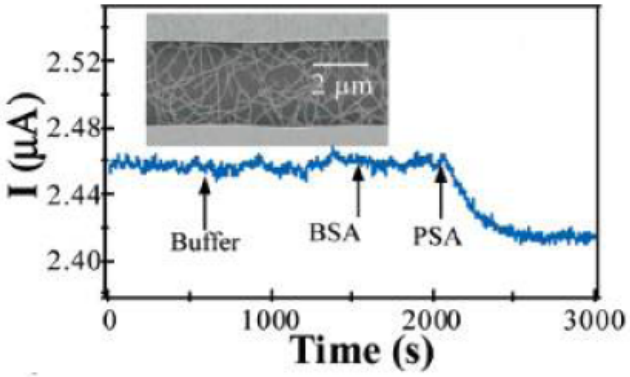

Additions for both devices:

1 drop of buffer: **No change**

100 nM BSA in PBS: **No change**

NW device:

140 pM (5 ng/mL) of PSA: **Current up by 1.3%**

Note:

S/N ~20. Detection limit could approach **250 pg/mL (7 pM)**.

SWNT device:

1.4 nM (50 ng/mL) of PSA: **Current down by 2%**

Note:

S/N ~5. Detection limit could approach **10 ng/mL (300 pM)**.

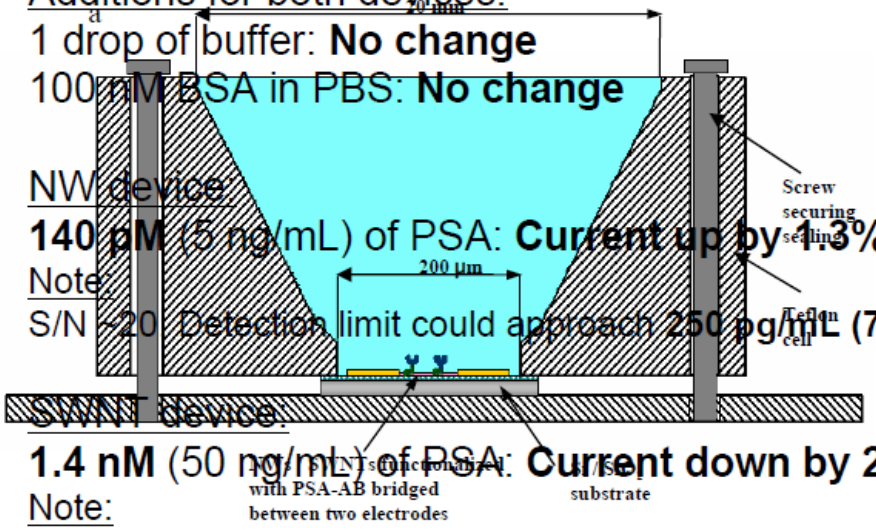

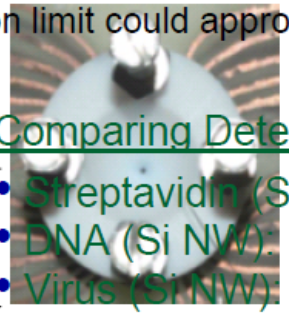

microfluidic channel

Comparing Detection Limit for:

- Streptavidin (Si NW): 10 pM
- DNA (Si NW): 10 fM
- Virus (Si NW): Single virus
- IgG protein (SWNT): 10 nM

C. Li, *et.* al. *J. Am. Chem Soc.*, **2005**

Array of 24 transistors

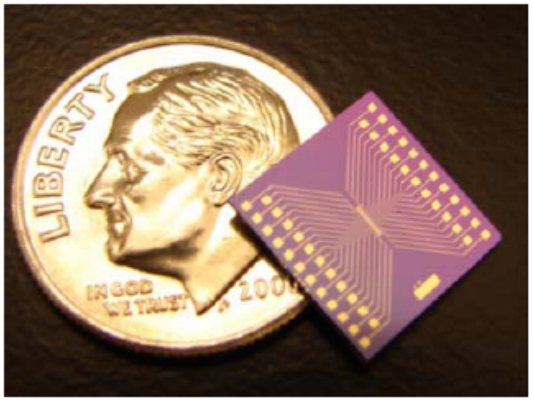

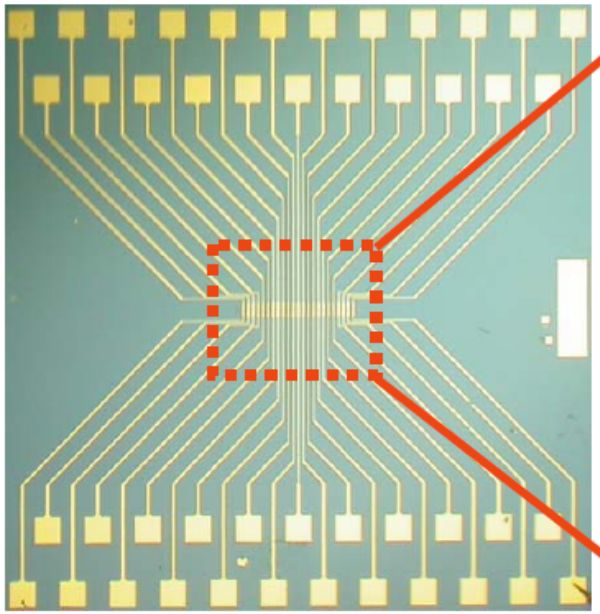

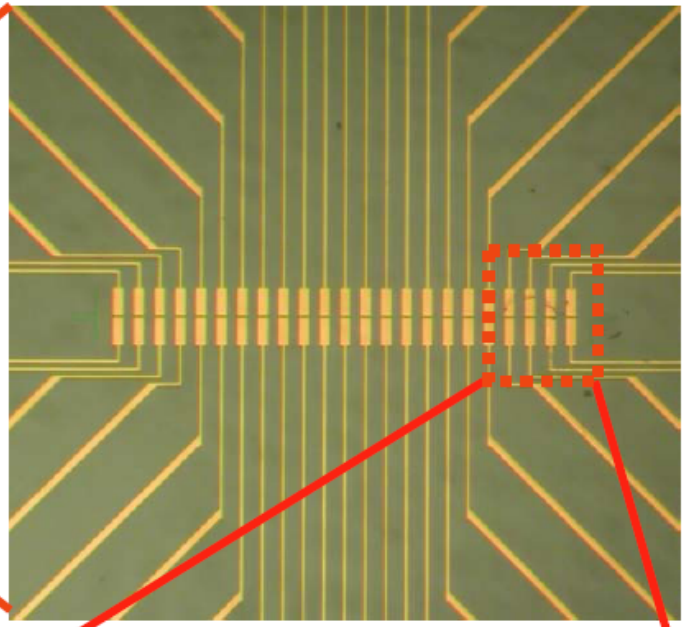

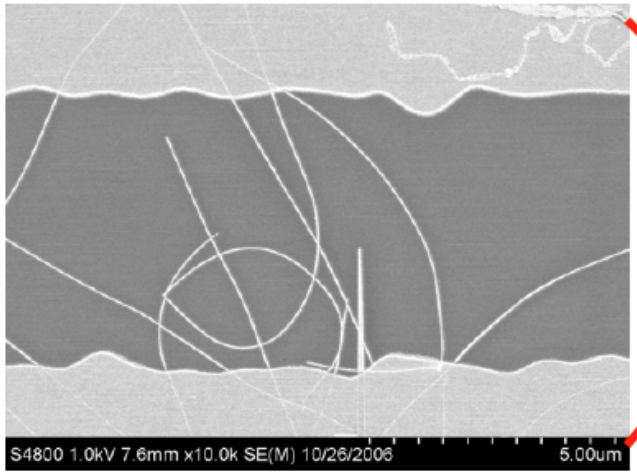

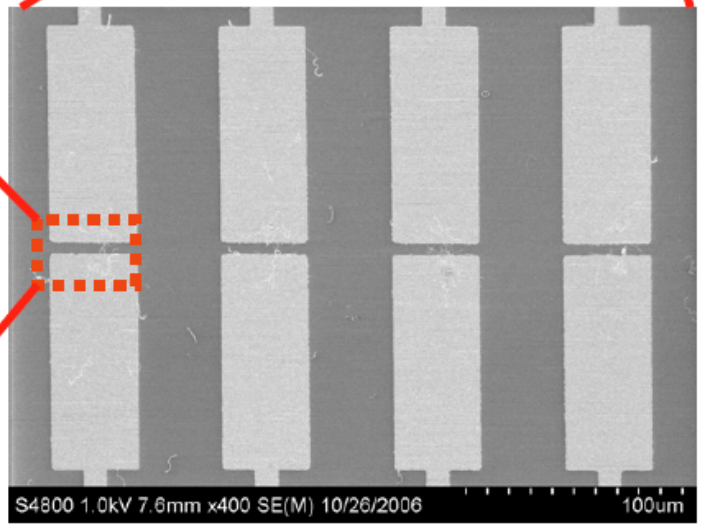

24 sensor array for coupling with microfluidic delivery

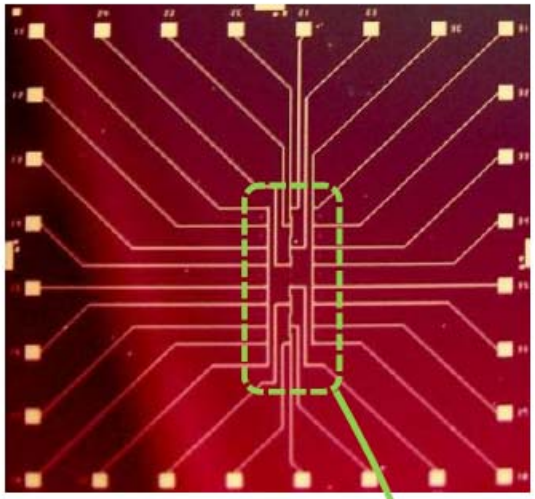

+

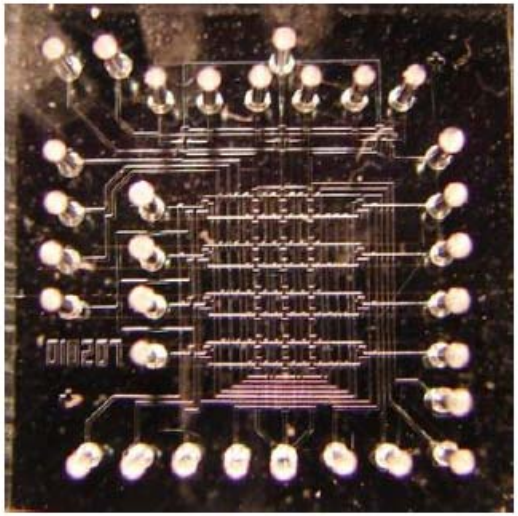

=

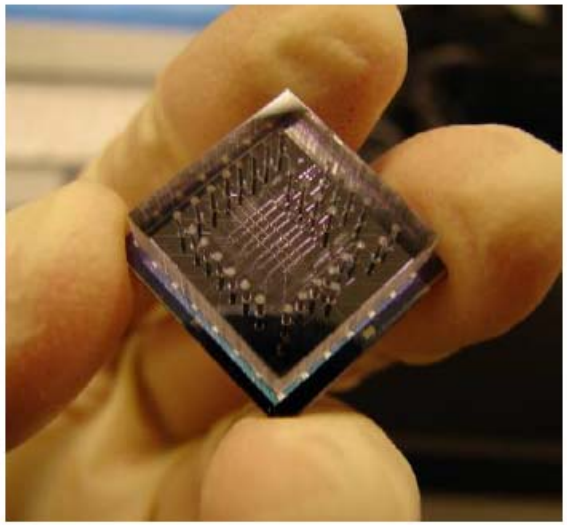

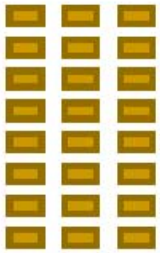

FET array design gives 3 rows of eight devices to match PDMS microflidic system

Integration of the Microfluics with the Nanosensors

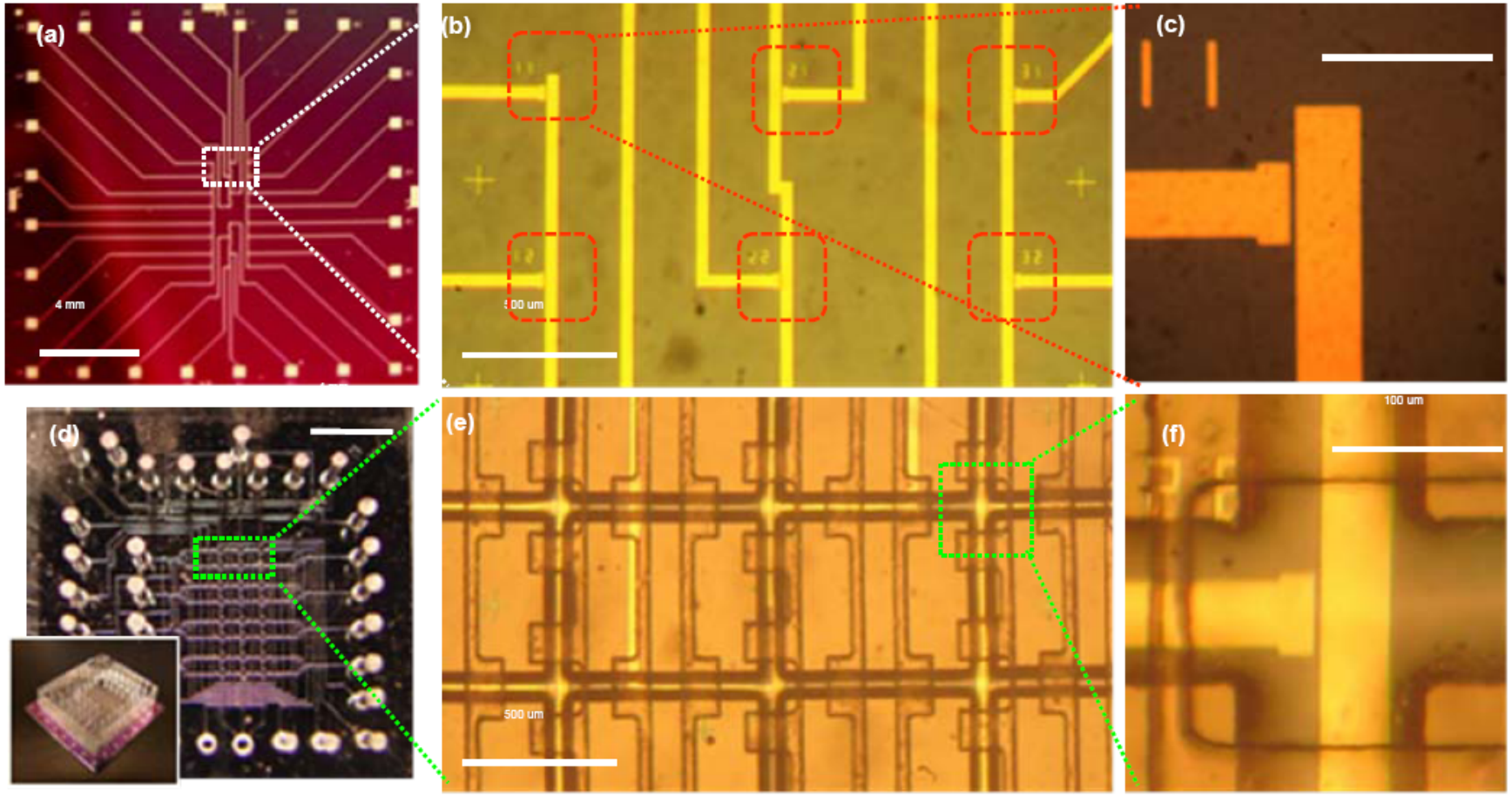

Functional microfluidics

Microfluidic Flow Diagram

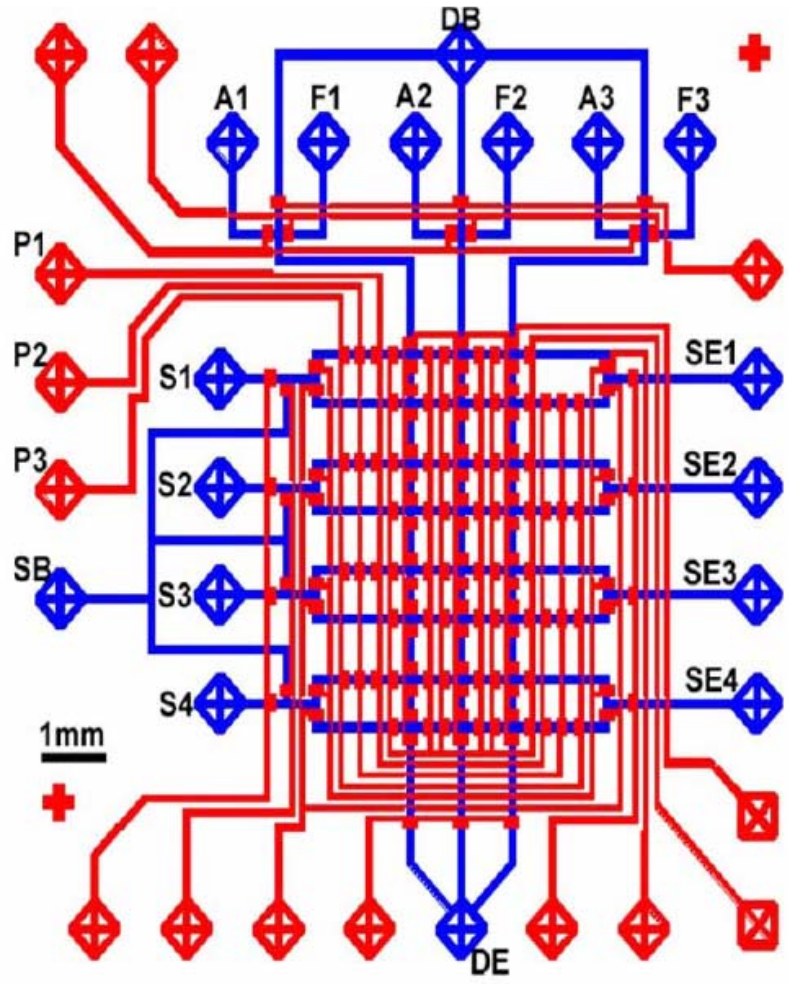

24 Identical Sensors

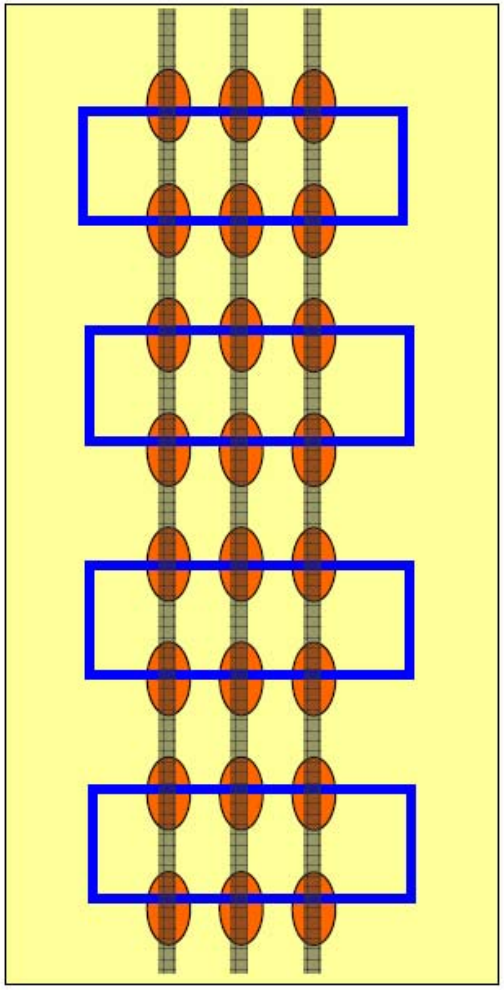

Multiplexed sensor arrays

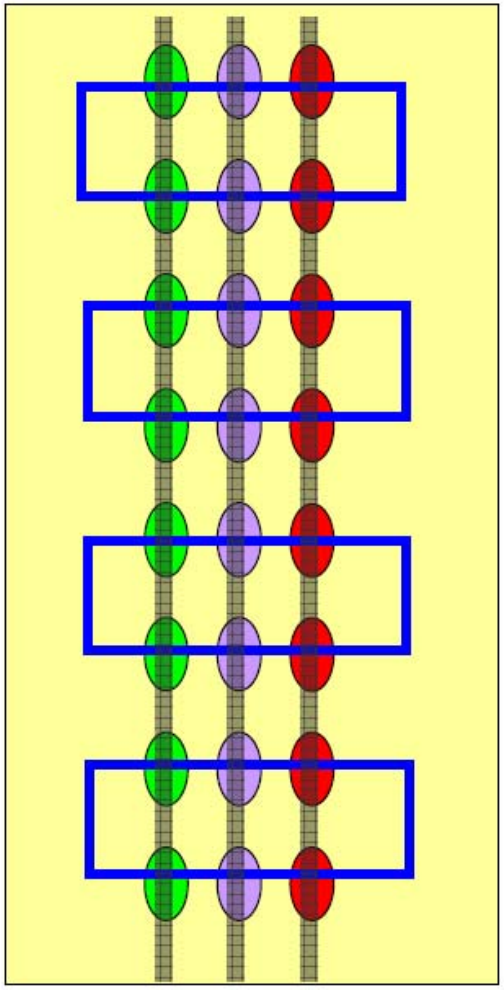

Latest Generation of Devices:

Problem: low density of nanowires on the substrate gives a variable number of NWs in each device: poor yield and uniformity

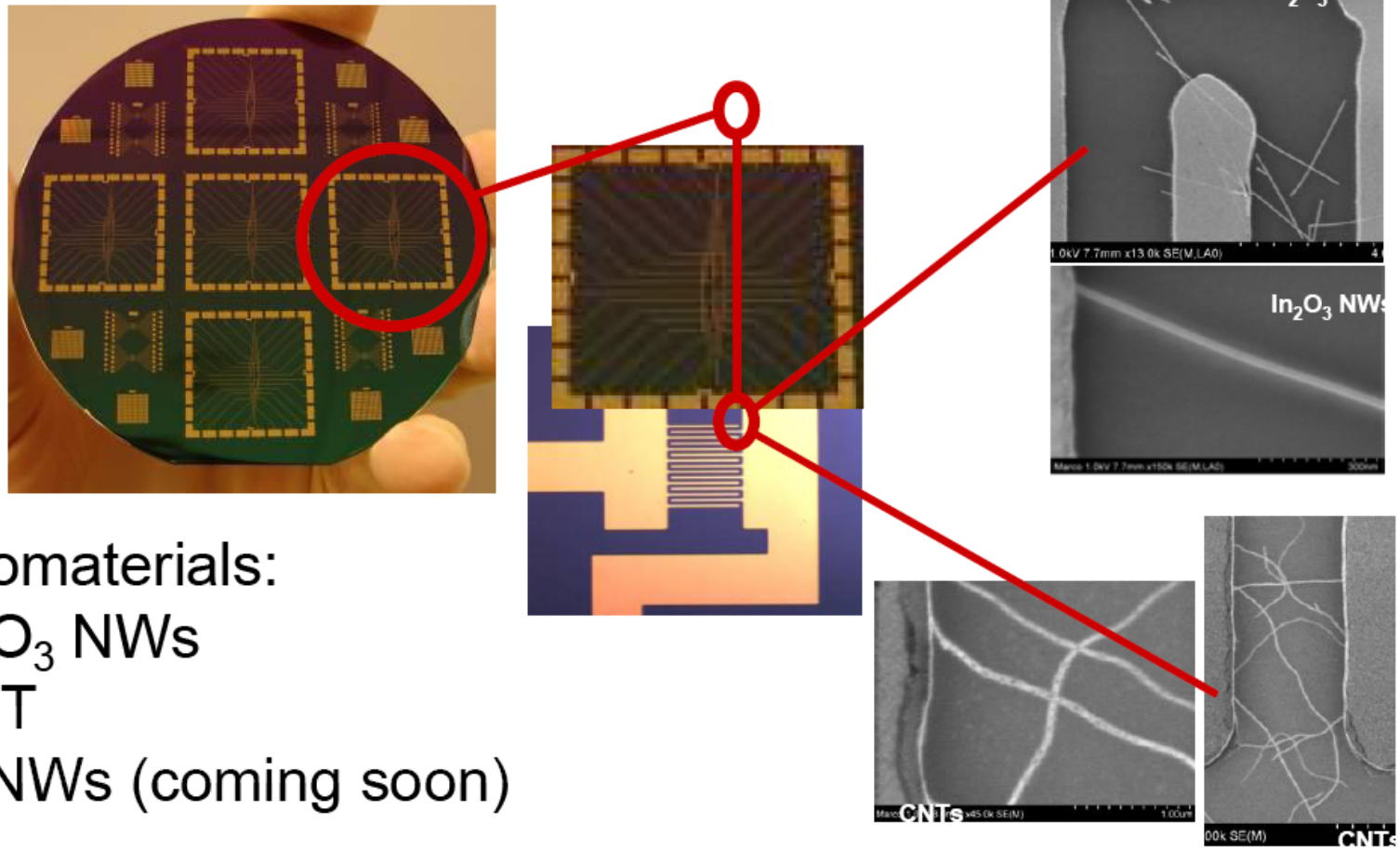

Nanomaterials:

- In_2O_3 NWs
- CNT
- Si NWs (coming soon)

Nanobiosensor array studies: next issues to attack

- Yield of active devices in the array
- Uniformity in response
  - Multiple device testing and statistical analysis
- Serum: selectivity versus sensitivity (?)
  - ELISA assay
  - Onboard filtration and separation
- Multiplexing
  - Microfluidic device selection and treatment
  - Chemical approaches to device selective treatment
- Lifetime and shelf life TBD

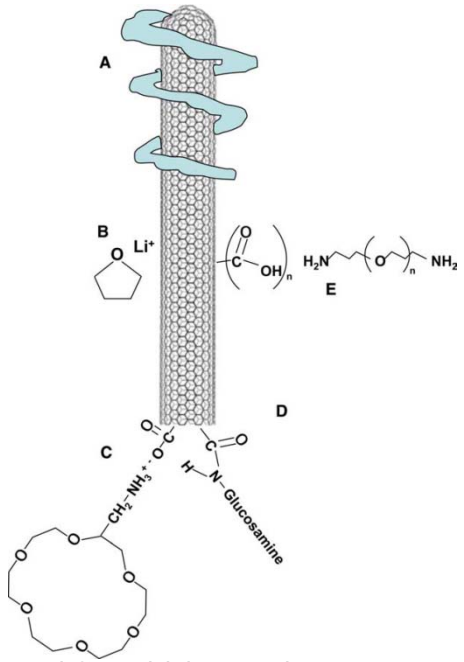

Schematic of typical CNT solubilization alternatives: (A) supramolecular wrapping with polymer; (B) CNT-Li+ conducting polyelectrolyte; (C) with amino group of 2-aminomethyl-18-crown-6 ether; (D) by amide bonds with glucosamine; and, (E) by diamine-terminated oligomeric poly(ethylene glycol). For details, see text and Table 1.\

Integration of carbon nanotubes

CNTs can be integrated into a variety of configurations to perform electrochemical detections. The current formats can be classified in groups:

- individual CNT configurations
- conventional electrodes that are modified with
- CNTs, in both oriented or non-oriented configurations and,
- CNTs integrated into a polymer matrix, creating a
- CNT composite

Trends

Trends in Analytical Chemistry, Vol. 24, No. 9, 2005

New materials for electrochemical sensing VI: Carbon nanotubes

Arben Merkoçi, Martin Pumera, Xavier Llopis, Briza Pérez, Manel del Valle, Salvador Alegret

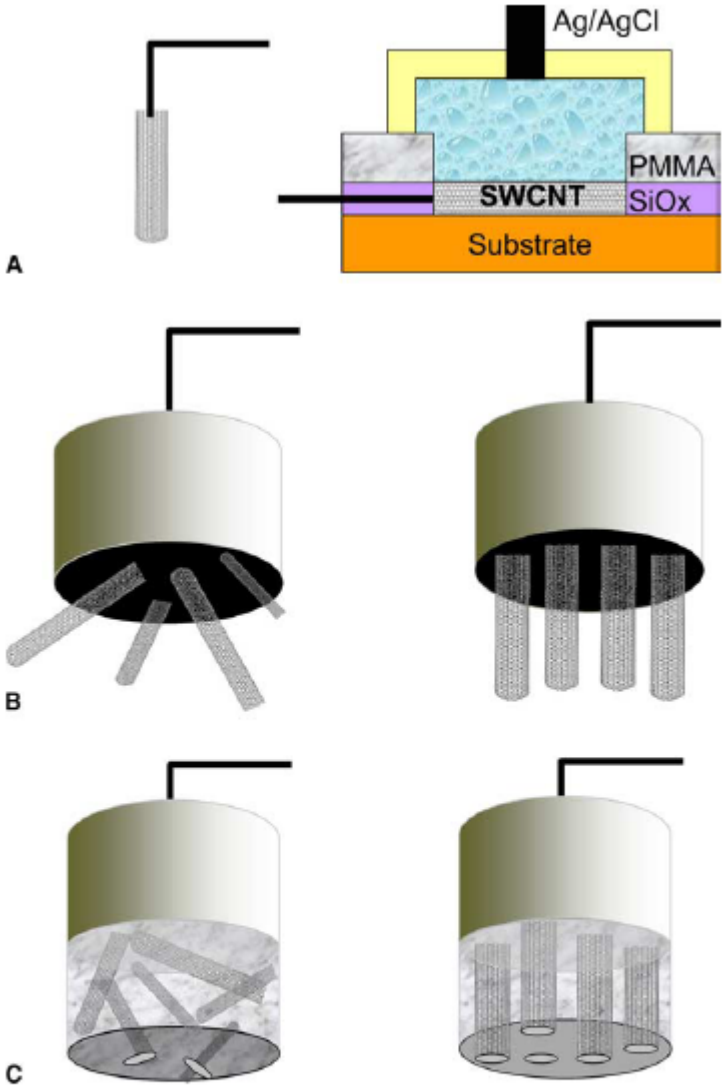

Figure 3. Three configurations of CNT integration in electrochemical sensors. (A) Use of individual CNT: for AFM tips (left) or individual SWCNT onto a Si wafer substrate (right). SiOx and PMMA are used as insulating layers in which windows are opened to expose the SWCNT; (B) electrode surface modifiers: non-oriented (left) and oriented (right) CNT configuration; and, (C) composites with non-oriented (left) and oriented (right) CNT configuration.

CNTs as modifiers of electrode surfaces

CNTs – both non-oriented (random mixtures, see left) and oriented (vertically aligned) –have been used to modify several conventional electrod surfaces, glassy carbon being the most reported.

5.2.1. Oriented modifications. The open end of an MWCNT has a fast electron transfer rate (ETR) similar to a graphite edge-plane electrode, while the SWCNT presents a very slow ETR and low specific capacitance, similar to the graphite basal plane [47]. Based on that idea, Li et al. [48] believed that the proper construction and orientation of the electrode is critical for its electrochemical properties. For that reason, they used a bottom-up approach, which is compatible with Si-microfabrication processes. They combined microlithography and nanolithography with catalytic CNT-growth techniques. A forest-like vertically aligned MWCNT array was grown on Ni-catalyst film using plasma-enhanced CVD. A dielectric encapsulation was then applied, leaving only the very end of CNTs exposed to form inlaid nanoelectrode arrays. The electrical and electrochemical properties of this oriented MWCNT array for small redox molecules have been characterized (by cyclic voltammetry and electrochemical impedance spectroscopy), showing well-defined quasi-reversible nanoelectrode behavior and ultrasensitive detection. Palleschi et al. [49] fabricated tungsten microelectrodes coated with homogeneous layers of SWCNTs. The coating

5.2.2. Non-oriented modifications. CNTs have been used to modify the surface of a conventional glassy-carbon electrode (GCE). The first use of CNTs was based on modifying GCEs with CNTs dispersed in sulphuric acid [50]. Prior to the surface modification, the GCE polished with alumina slurries and washed was cast with 10 μL of a concentrated solution of CNT in sulphuric acid (1 mg CNT/mL). The coated electrode was dried at 200°C for 3 h and it was then ready to be used after careful washing. GCEs were also modified with CNTs using three other dispersing agents: dimethylformamide (DMF), concentrated nitric acid or a Nafion/water mixture [51]. In all cases, the CNTs were purified prior to use by nitric acid solution for 20 h to ensure complete removal of metal catalysts from the CNTs. The CNT-casting solutions were dropped directly onto the glassy carbon surface and allowed to dry. The electrode was then ready for use. The authors found differences in the electrochemical reactivity between the CNT-modified electrodes and the control electrodes (glassy carbon treated in the same way but without CNTs). They attributed this difference

5.3.2. Teflon. CNT/Teflon composite electrodes were prepared in the dry state by hand-mixing the desired amounts of CNTs with granular Teflon [57]. A portion of the resulting consolidated composite was packed firmly into the electrode cavity forming the electrode. The authors did not observe redox activity for peroxide and NADH at the conventional graphite/Teflon control electrode using potentials lower than 0.6 and 0.5 V, respectively. The control graphite/Teflon electrode showed only a small gradual increase of response at higher potentials. By contrast, the CNT/Teflon electrode

5.3. Pastes and composites

Carbon-paste (CP) and composite electrodes have been used in electrochemical sensors for several years. By analogy, similar matrices that involve CNTs have recently been one of the focuses of research in the field of electrochemical sensors. CNTs inside the polymer matrix can be distributed oriented either randomly (Fig. 3C left) or vertically (Fig. 3C, right). A variety of binders (e.g., mineral oil, Teflon or epoxy resins) to produce CNT pastes or composites were reported, with rigid epoxy-based CNT composites being the least exploited.

5.3.1. Mineral oil. SWCNT paste electrodes can be obtained by mixing CNTs with a mineral oil binder [56]. The high surface area of CNTs makes possible the construction of stable, robust paste electrodes with high amounts of mineral oil (50% CNTs and 50% mineral oil). Such high mineral oil loadings are not possible when a conventional graphite-powder CP electrode (CPE) is prepared, since it results in the CPE leaking into the solution. The electrochemistry of CNT paste electrodes (CNTPEs) for ferricyanide, sodium hexachloroiridate(III) hydrate, catechol, dopamine, serotonin 5-HT, and caffeic acid was improved significantly compared to that of conventional CPEs. According to the authors, the electro-

6. Coupling with biological molecules

6.1. Enzymes

One of the key issues in biosensor design is the establishment of a fast electron-transfer between the active site of the enzyme and the electrochemical transducer. This is a significant challenge in designing enzyme-based sensors, taking into consideration the additional restrictions applied when miniaturization of the device is attempted.

The majority of reported articles (see Section 5) have demonstrated that CNTs promote electron-transfer reactions at low overpotentials (see Table 2). This advantage has inspired increased research in coupling CNT-based sensors with enzymes.

Glucose is one of the most reported analytes detected *via* enzyme–CNT electrodes. Several strategies were used to immobilize the necessary enzymes. Glucose oxidase (GOx) has been immobilized onto CNTs *via* polypyrrole [59,60] or even through CNT inks [61].

Glucose dehydrogenase (GDH) has been covalently immobilized in the CNT–CHIT (Chitosan) films using glutaric dialdehyde (GDI) [51]. The stability and the sensitivity of the GC electrode modified with CNT–CHIT–GDI–GDH biosensor allowed interference-free determination of glucose in the physiological matrix.

Table 2. Reported cyclic voltammetric peak-to-peak separations and oxidative peak potentials for CNT-based electrodes

CNT/length/source	CNT solubilization solvent/immobilization matrix	Control electrode	Analyte	Oxidation potential/peak-to-peak separation[a,b]		Potential shift (V)	Reference
				CNT electrode (V)	Control electrode (V)		
SWCNTs deposited by CVD onto tungsten wire	–	Glassy carbon	$Fe(CN)_6^{3-/4-}$	0.31[a]	0.32[a]	0.01	[49]
SWCNT/–/CVD Nanolab	H_2SO_4/film	Glassy carbon	NADH	0.32[a]	0.82[a]	0.50	[50]
MWCNT/–/CVD Nanolab			NADH	0.33[a]	0.82[a]	0.49	
MWCNT/1–5 μm/CVD Nanolab	DMF/film	Glassy carbon	$Fe(CN)_6^{3-/4-}$	0.43[a]	0.70[a]	0.27	[51]
			H_2O_2	0.40[a]	0.65[a]	0.25	
			NADH	0.43[a]	0.70[a]	0.27	
MWCNT/1–5 μm/CVD Nanolab	Nitric acid/film	Glassy carbon	$Fe(CN)_6^{3-/4}$	0.43[a]	1.00[a]	0.57	[51]
MWCNT/5–20 μm/CVD Nanolab			H_2O_2	0.48[a]	0.75[a]	0.27	
MWCNT/1–5 μm/CVD Nanolab			NADH	0.43[a]	1.00[a]	0.57	
MWCNT/1–5 μm/CVD Nanolab	Nafion/film	Glassy carbon	H_2O_2	0.37[a]	0.54[a]	0.17	[51]
MWCNT/–/Nanolab	Chitosan/film	Glassy carbon/ chitosan	NADH	0.34[a]	0.60[a]	0.26	[52]
CNT formed *in situ* onto Au substrate	Polypyrrole/film	Au/PPy	H_2O_2	0.20[a]	0.65[a]	0.45	[59]
MWCNT/1–5 μm/CVD Nanolab	DMF/film	Glassy carbon	H_2S	−0.30[a]	0.10[a]	0.40	[90]
MWCNT/Arc method produced			H_2S	0.00[a]	0.10[a]	0.10	
MWCNT	Acetonitrile/film	Glassy carbon and graphite powder	$Fe(CN)_6^{3-/4}$	0.146[b]	0.167[b]	–	[53]
			Norepinephrine	0.30[a]	0.29[a]	−0.01	
			NADH	0.52[a]	0.56[a]	0.04	
			Epinephrine	0.44[a]	0.48[a]	0.04	
SWCNT/Sigma	Mineral oil/paste	Carbon paste	$Fe(CN)_6^{3-/4}$	0.090[b]	0.209[b]	–	[56]
			Na_2IrCl_6	0.120[b]	0.090[b]	–	
			$Ru(NH_3)_6$	0.094[b]	0.092[b]	–	
			Ferrocyanic acid	0.060[b]	0.060[b]	–	
			Catechol	0.239[b]	0.344[b]	–	
			Dopamine	0.164[b]	0.149[b]	–	
			Caffeic acid	0.422[b]	0.299[b]	–	
MWCNT/–/Merck Inc	Teflon binder/paste	Graphite–Teflon composite	H_2O_2	0–1.0[a]	0.6–1.0[a]	0–0.4	[57]
			NADH	0–1.0[a]	0.5–1.0[a]	0–0.5	
MWCNT/0.5–2 μm/Sigma	Epoxy/composite	Graphite–epoxy composite	$Fe(CN)_6^{3-/4}$	0.302[b]	0.369[b]	–	[58]
MWCNT/0.5–200 μm/Sigma			$Fe(CN)_6^{3-/4}$	0.211[b]	0.369[b]	–	
MWCNT/0.5–2 μm/Sigma			NADH	0.72[a]	0.74[a]	0.02	
MWCNT/0.5–200 μm/Sigma			NADH	0.45[a]	0.74[a]	0.29	
MWCNT/0.5–2 μm/Sigma			H_2O_2	0.60[a]	No clear peak	–	
MWCNT/0.5–200 μm/Sigma			H_2O_2	0.50[a]	No clear peak	–	

[a,b] – values marked with "a" correspond to the oxidation potential, while values marked with "b" correspond to CV peak-to-peak separation.

To achieve a fast electron-transfer (i.e., in the case of glucose oxidase) between the redox active site of the enzyme – flavin adenine dinucleotide (FAD) – and the transducing electrode, CNT-modified gold electrodes have been used [62,63] (see Fig. 5). Gold electrodes were first modified with a self-assembled monolayer of cysteamine and then short SWCNTs were aligned normal to the electrode surface by self-assembly. The CNTs were plugged into the enzymes in two ways:

- native glucose oxidase was covalently attached to the ends of the aligned tubes which allowed close approach to FAD and direct electron transfer was observed with a rate constant of 0.3/s; and,
- FAD was attached to the ends of the tubes and the enzyme reconstituted around the surface immobilized FAD. This latter approach allowed more efficient electron transfer to the FAD with a rate constant of 9/s.

According to Gooding [63], advantages of these electrode arrays are:

- the electroactive ends of the nanotubes are readily accessible to species in solution; and,
- the rigidity of the tubes allows them to be plugged into biomolecules, so enabling electrical connection to the redox centers of the biomolecules.

Biosesenors have been based on other enzymes, such as acetylcholinesterase (AChE) [64] immobilized through a CNT-modified thick-film strip electrode for organophosphorus insecticides, horseradish peroxidase (HRP) [65] attached covalently onto the ends of SWCNTs, or L-amino acid oxidase [66] incorporated *via* an alkoxy silane sol–gel process. The sol–gel process has been also reported for coupling urease or acetylcholinesterase activity with CNT electrochemical transduction [67].

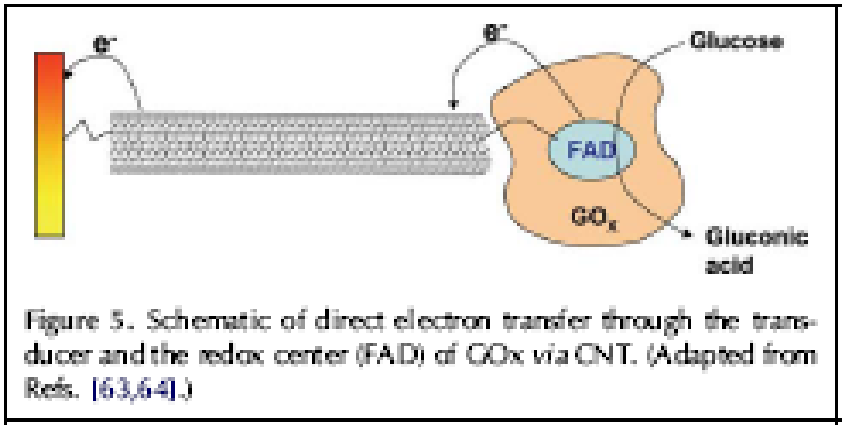

Figure 5. Schematic of direct electron transfer through the transducer and the redox center (FAD) of GOx *via* CNT. (Adapted from Refs. [63,64].)

Biosesenors have been based on other enzymes, such as acetylcholinesterase (AChE) [64] immobilized through a CNT-modified thick-film strip electrode for organophosphorus insecticides, horseradish peroxidase (HRP) [65] attached covalently onto the ends of SWCNTs, or L-amino acid oxidase [66] incorporated *via* an alkoxy silane sol–gel process. The sol–gel process has been also reported for coupling urease or acetylcholinesterase activity with CNT electrochemical transduction [67].

CNTs may even play a dual-amplification role in both recognition and transduction events. This is demonstrated in high-sensitivity DNA detection, where CNTs have been loaded with numerous enzyme tags and used as DNA labels during hybridization detection (see Fig. 6B) [70]. Beside enzyme loading, the CNTs participate in accumulating the product of the enzymatic reaction, enhancing the DNA signal. These novel support and preconcentration functions of CNTs reflect their large specific surface area and are illustrated using the alkaline phosphatase (ALP) enzyme tracer. Such coupling of several CNT-derived amplification processes leads to the lowest detection limit reported for electrical DNA detection. A similar loading effect was also demonstrated earlier with quantum dots as electroactive labels for DNA-hybridization detection (Fig. 6C) [71].

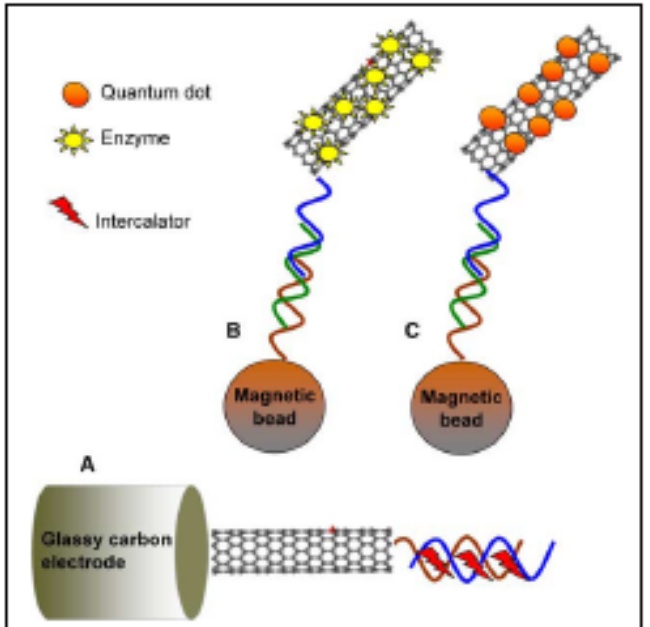

Figure 6. DNA detection via CNT. (A) direct electron transfer via intercalator; (B) CNT loaded with enzymes; and, (C) CNT loaded with quantum dots.

6.3. *Proteins*

Following the same strategy as for DNA (see Section 6.2), it was also possible to detect proteins [69] by using CNTs as reservoirs of enzyme molecules and at the same time to accumulate the products coming from the enzymatic reaction during a complete sandwich-detection scheme (see Fig. 7A).

Wohlstadter et al. [72] immobilized biotinylated anti-AFP (alpha-feto protein) antibodies on the surface of a streptavidin-coated CNT composite using poly(ethylene)-vinylacetate as binder and they exposed this derivatized composite to a sample containing AFP and anti-AFP antibodies conjugated with colloidal gold or $Ru(bpy)_3^{2+}$ (Fig. 7B). The sandwich immunoassay was biospecific, and this was verified by SEM and electrochemical-luminescence (ECL) measurements. The ECL signal was found to be linearly dependent on AFP concentration up to concentrations of 30 nM. This work shows that CNTs can be used as immobilization platform and working electrode at the same time. The CNT-modification procedure (based on covalent coupling of streptavidin) can be extended to electrochemical-detection procedures based on voltammetric measurements, including those involving enzymes as markers.

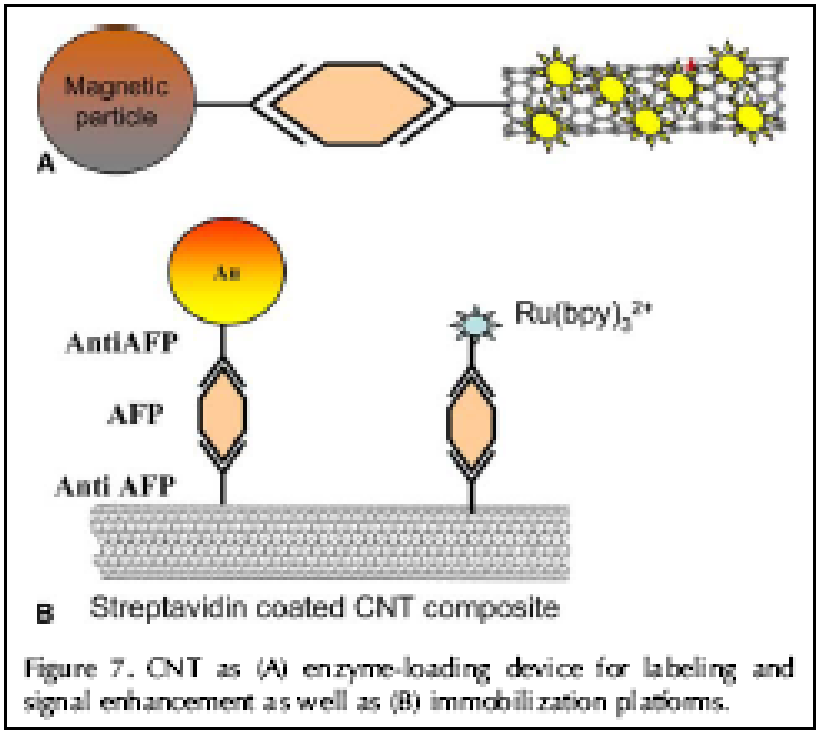

Figure 7. CNT as (A) enzyme-loading device for labeling and signal enhancement as well as (B) immobilization platforms.

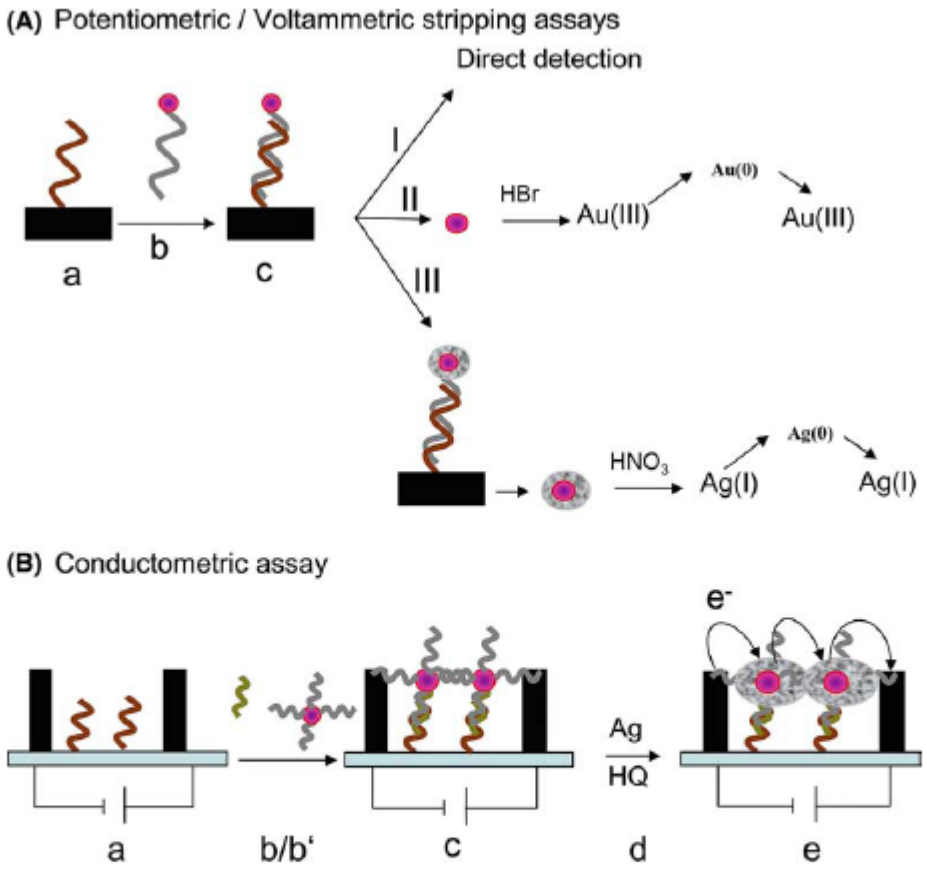

Figure 5. Detection strategies of gold nanoparticles. (A) Potentiometric/voltammetric stripping assay. The hybridization event occurs between DNA strand (a) and gold-tagged DNA (b). The gold-labeled duplex (c) formed is then detected according to each strategy: (i) direct detection of the nanoparticles onto the bare electrode without the need for tag dissolution; (ii) the gold nanoparticles are dissolved with HBr/Br_2 treatment and then detected by stripping techniques; and, (iii) The gold nanoparticles are first covered with Ag by a deposition treatment and then detected by stripping techniques *via* silver enhanced signal. (B). Conductivity assay. Probe DNA immobilized in a small gap between two electrodes (a) is hybridized with target DNA (b) and then with gold-modified DNA probes (b'). Gold is accumulated in the gap (c). Silver enhancement (d) is performed in the presence of hydroquinone (HQ). The silver precipitated onto the gold nanoparticles (e) improves the sensitivity of the assay by lowering the resistance across the electrode gap.

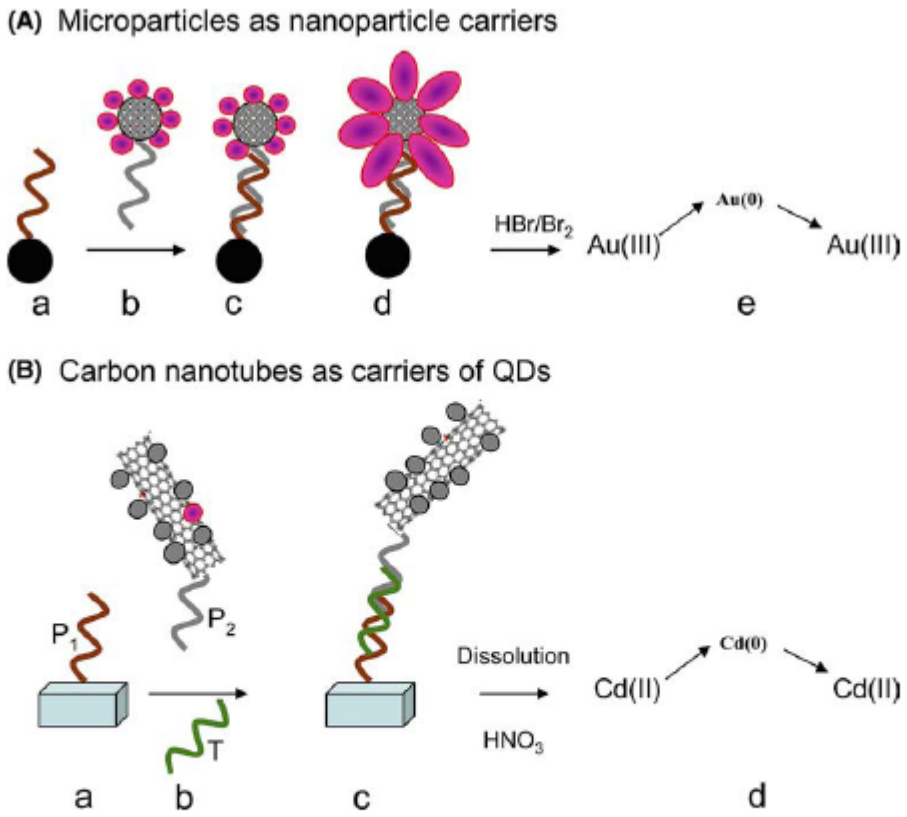

Figure 6. (A) Microparticles as nanoparticle carriers. The target DNA immobilized onto magnetic beads (a) hybridizes with the nucleic acid functionalized with Au-nanoparticle-carrier polystyrene beads (b) forming the Au-labeled hybrid (c) the tags of which are than enlarged (d) followed by magnetic separation and a dissolution process with HBr/Br_2 and then detection by stripping voltammetry (e). (B) Carbon nanotubes as carriers of QDs. The DNA probe P1 is first immobilized onto the well of a streptavidin-assay plate (a). The DNA target (T) and the single wall carbon nanotube (SWCNT)–CdS–labeled probe (P2) were then added, followed by a dual hybridization event (b) forming the final CdS-tagged sandwich (c). The QDs are dissolved with 1 M HNO_3 and then detected by stripping voltammetry using a mercury-coated glassy carbon electrode (d).

Semiconductor quantum dots

The foremost application of quantum dots (QDs) as sensors is based on the Forster resonance energy transfer effect (FRET). Owing to this effect, the fluorescence emanating from QDs changes from an ON state to an OFF state.

FRET takes place when the electronic excitation energy of a donor fluorophore is relocated to a neighbouring acceptor molecule without exchanging light between the donor and the acceptor.

Goldman *et al.* (2004), used QDs functionalized with antibodies to perform multiplexed fluoroimmunoassays for simultaneous detection of various toxins. This type of sensor could be used for environmental purposes for concurrently recognizing pathogens like cholera toxin or ricin in water.

The FRET principle was also applied to a maltose biosensor. The sensing mechanism was the application of semiconductor QDs conjugated to a maltose binding protein covalently bound to a FRET acceptor dye. In absence of maltose, the dye occupied the protein binding sites. Energy transference from the QDs to the dyes quenched the QD fluorescence. When maltose was present, it replaced the dye leading to recovery of the fluorescence.

Quantum-dot-tagged microbeads for multiplexed optical coding of biomolecules

Mingyong Han, Xiaohu Gao, Jack Z. Su, and Shuming Nie*

Multicolor optical coding for biological assays has been achieved by embedding different-sized quantum dots (zinc sulfide–capped cadmium selenide nanocrystals) into polymeric microbeads at precisely controlled ratios. Their novel optical properties (e.g., size-tunable emission and simultaneous excitation) render these highly luminescent quantum dots (QDs) ideal fluorophores for wavelength-and-intensity multiplexing. The use of 10 intensity levels and 6 colors could theoretically code one million nucleic acid or protein sequences. Imaging and spectroscopic measurements indicate that the QD-tagged beads are highly uniform and reproducible, yielding bead identification accuracies as high as 99.99% under favorable conditions. DNA hybridization studies demonstrate that the coding and target signals can be simultaneously read at the single-bead level. This spectral coding technology is expected to open new opportunities in gene expression studies, high-throughput screening, and medical diagnostics.

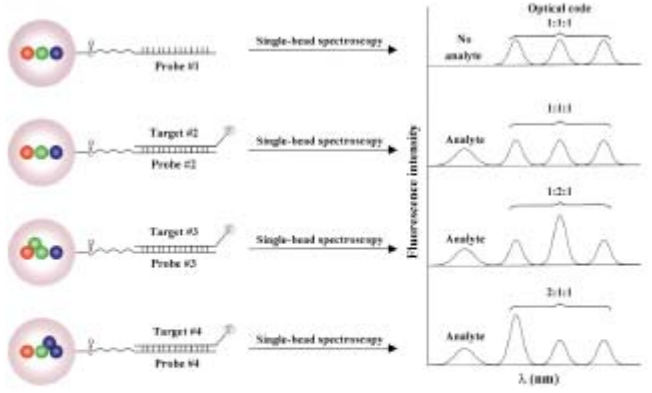

Figure 5. Schematic illustration of DNA hybridization assays using QD-tagged beads. Probe oligos (No. 1–4) were conjugated to the beads by cross-linking, and target oligos (No. 1–4) were detected with a blue fluorescent dye such as Cascade Blue. After hybridization, nonspecific molecules and excess reagents were removed by washing. For multiplexed assays, the oligo lengths and sequences were optimized so that all probes had similar melting temperatures (T_m = 66°–99°C) and hybridization kinetics (30 min). See legend in Figure 6 for the sequences used.

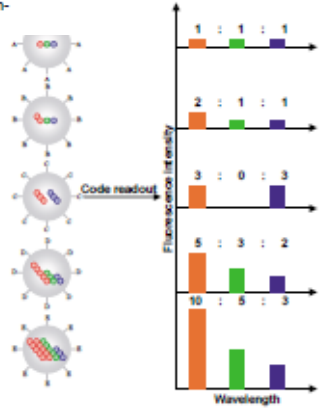

B

Figure 1. (A) Schematic illustration of optical coding based on wavelength and intensity multiplexing. Large spheres represent polymer microbeads, in which small colored spheres (multicolor quantum dots) are embedded according to predetermined intensity ratios. Molecular probes (A–E) are attached to the bead surface for biological binding and recognition, such as DNA–DNA hybridization and antibody–antigen/ligand–receptor interactions. The numbers of colored spheres (red, green, and blue) do not represent individual QDs, but are used to illustrate the fluorescence intensity levels. Optical readout is accomplished by measuring the fluorescence spectra of single beads. Both absolute intensities and relative intensity ratios at different wavelengths are used for coding purposes; for example (1:1:1) (2:2:2), and (2:1:1) are distinguishable codes. (B) Ten distinguishable emission colors of ZnS-capped CdSe QDs excited with a near-UV lamp. From left to right (blue to red), the emission maxima are located at 443, 473, 481, 500, 518, 543, 565, 587, 610, and 655 nm.

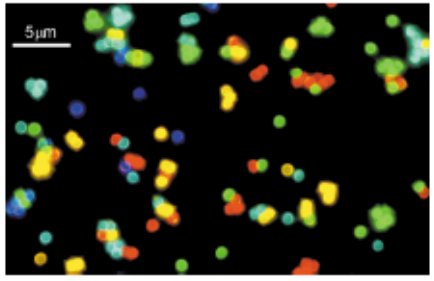

Figure 2. Fluorescence micrograph of a mixture of CdSe/ZnS QD-tagged beads emitting single-color signals at 484, 508, 547, 575, and 611 nm. The beads were spread and immobilized on a polylysine-coated glass slide, which caused a slight clustering effect. See Experimental Protocol for detailed conditions.

tinguishable. As noted earlier, this type of simultaneous excitation is not possible with fluorescent microspheres containing organic dyes. Confocal imaging studies indicate that the QDs are mainly located in the outer 25% of the bead's radius, similar to the spatial distribution of organic dyes in polystyrene beads[25]. However, this determination is only an approximate estimate because the microbeads refract light and cause image distortion.

A key question is whether the embedded QDs would aggregate and couple with each other inside the beads, which could cause spectral broadening, wavelength shifting, and energy transfer. To our surprise, the fluorescence spectra of QD-tagged beads are narrower by ~10% than those of free QDs, and the emission maxima remain unchanged. We believe that the bead's porous structure acts as a matrix to spatially separate the embedded QDs, and also as a filter to block the incorporation of large particles and aggregates in a heterogeneous population. Our calculation indicates that the average distance between two adjacent QDs is ~30 nm within a 1.2-μm bead that contains 50,000 QDs (~0.1% vol/vol, corresponding to the maximum level of QD incorporation). Despite the uneven nature of QD distribution within the beads, this calculation suggests that the average separation distance is much larger than the Förster energy transfer radius (R_0 = 5–8 nm) for QDs (refs 26,27).

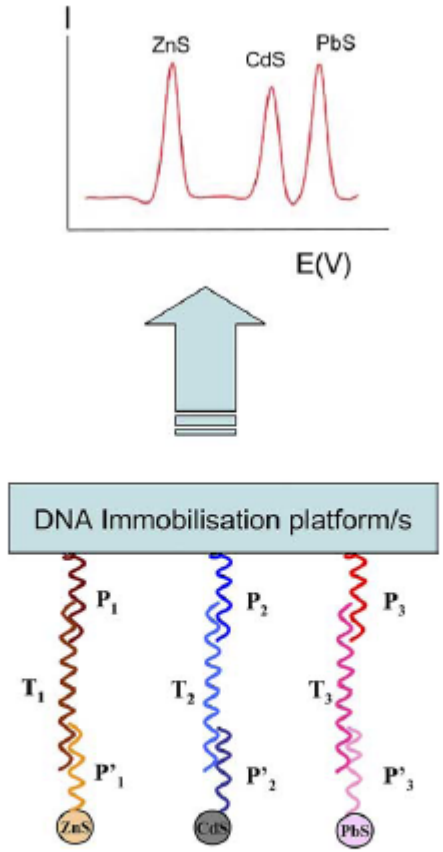

Figure 7. Schematic of multiple detection of DNA. DNA probes (P′1, P′2 and P′3) bearing different DNA sequences with different nanoparticles (ZnS, CdS and PbS, respectively) that enable the simultaneous detection of three DNA targets (T1, T2 and T3) hybridized with corresponding DNA-capturing probes (P1, P2 and P3) immobilized onto a direct or an indirect (magnetic particles) transducing platform/s.

The labeling of probes bearing different DNA sequences with different nanoparticles enables the simultaneous detection of more than one target in a sample, as shown in Fig. 7. The number of targets that can be readily detected simultaneously (without using high-level multiplexing) is controlled by the number of voltammetrically distinguishable nanoparticle markers. A multi-target sandwich hybridization assay involving a dual hybridization event, with probes linked to three tagged inorganic crystals and to magnetic beads has been reported [46]. The DNA-connected QDs yielded well-defined and resolved stripping peaks at −1.12 V (Zn), −0.68 V (Cd) and −0.53 V (Pb) at the mercury-coated glassy carbon electrode (vs. the Ag|AgCl reference electrode).

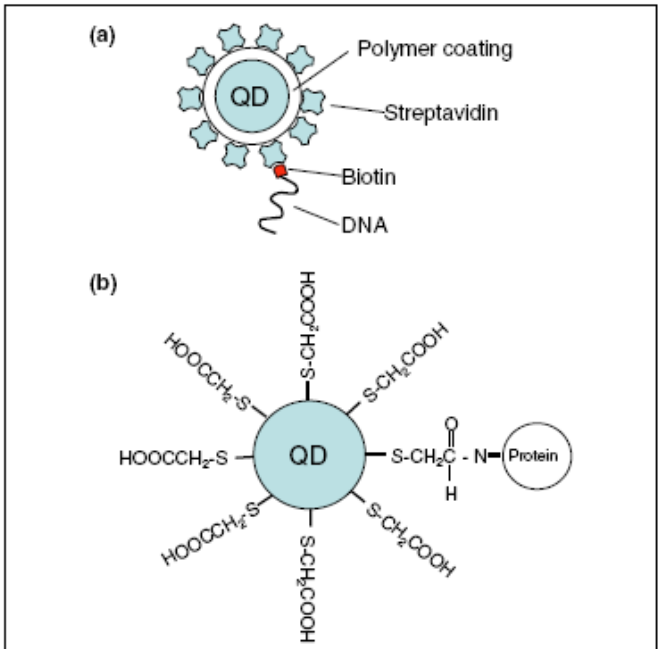

Figure 4. (a) A QD coated with a polymer modified with streptavidin. A biotin-functionalized DNA is attached onto the surface. (b) Schematic of a CdS QD that is covalently coupled to a protein through mercaptoacetic acid by using ethyl-3-(dimethyl-aminopropyl)carbodiimide) as a bifunctional reagent.

Table 1. Reported nanoparticle labels and analytical parameters of the assays developed

Nanoparticle label	Label connection with DNA	Detection technique	Hybridization separate from detection	DNA detection limits	RSD	Reference
Au	Au–SH–DNA	DPV at pencil-graphite electrode	No	0.78 fmol/mL	~8%	[37]
Au	Au–SH–DNA	PSA and silver catalytic enhancement at screen-printed electrodes	Yes	150 pg/mL	7%	[39,40]
Au	Au–SH–DNA	Conductivity at micro-electrodes	No	500 fM	–	[41]
Au carried into PVC beads	PVC (Au) strep-tavidin–biotin–DNA	PSA and silver catalytic enhancement at screen-printed electrodes	Yes	40 pg/mL	13%	[45]
CdS QDs	CdS NH–DNA	EIS with gold electrode	No	1.43×10^{-10} M	–	[44]
CNTs loaded with CdS QDs	CNT–CdS–strep-tavidin–biotin–DNA	DPV at Hg-film electrode	Yes	40 pg/mL	6.4%	[25]
Au–Fe (core/shell)	Fe–Au–SH–DNA	DPV at Hg-film electrode	Yes	50 ng/mL	6.3%	[43]
CdS QDs	CdS–SH–DNA	PSA and catalytic enhancement with Cd at screen-printed electrodes	Yes	20 ng/mL	6%	[42]
CdS QDs PbS QDs ZnS QDs	CdS–SH–DNA PbS–SH–DNA ZnS–SH–DNA	Simultaneous detection with SWV at Hg-film electrode	Yes	5 ng/mL	9.4%	[46]

PSA, Potentiometric stripping analysis; DPV, Differential pulse voltammetry; SWV, Square wave voltammetry; EIS, Electrochemical impedance spectroscopy.